Engineering Geology 338 (2024) 107614

Contents lists available at ScienceDirect

Engineering Geology

journal homepage: www.elsevier.com/locate/enggeo

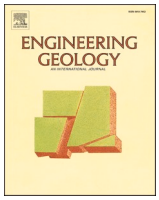

Simulating landslides with the material point method: Best practices, potentialities, and challenges

Francesca Ceccato [a,*], Alba Yerro [b], Gaia Di Carluccio [c]

[a] Department of Civil, Environmental and Architectural Engineering, Via Ognissanti 39, Padua, Italy University of Padova, Italy
[b] Virginia Polytechnic Institute and State University, Department of Civil and Environmental Engineering, 750 Drillfield Drive, 200 Patton Hall, Blacksburg, VA, United States
[c] International Centre for Numerical Methods in Engineering (CIMNE), C/ Gran Capità S/N UPC Campus Nord, 08034 Barcelona, Spain

ARTICLE INFO

Keywords:
Material point method
Landslides
Numerical simulation

ABSTRACT

Advances in numerical methods have provided useful tools for investigating the complex behaviour of landslides, which can be a valuable support for landslide hazard assessment, planning, and design of mitigation measures. Among different methodologies, the Material Point Method (MPM) has recently grown in popularity, thanks to its ability to simulate large displacements and has been applied to simulate an increasing number of real cases. Despite the success, there are still several challenges to be addressed. This paper aims to present the current state of the art in the modelling of real landslide case histories with MPM. The key numerical features used to capture the evolution of different types of landslides are discussed, such as constitutive models, soil-water interaction, and triggering mechanisms, thus providing insight into the computational aspects of using MPM to serve as guidelines for future applications. Limitations and future perspectives are also mentioned to encourage the development of new solutions for current numerical challenges and further extend the applicability of the methodology in this field.

1. Introduction

Landslides are dangerous natural hazards that involve different types of material and mobility mechanisms. In recent decades, significant advances have been made in understanding landslide mechanisms thanks to the developments in measurement and monitoring techniques, field tests, laboratory tests, and numerical studies.

One of the first methodologies proposed to investigate the stability of slopes is the Limit Equilibrium Method (LEM), which allows calculating a factor of safety (FS), commonly defined as the ratio between the maximum available shear strength and the mobilised shear stress. FS is generally calculated based on the equilibrium of driving and resistance forces, assuming an arbitrary shape of the failure surface and rigid-perfectly plastic soil behaviour. Since the 1950s, LEM has had wide applicability due to its simplicity, and it is still valuable to evaluate the proximity of slope failure. Furthermore, because of its small computational cost, it is well suited to be used in probabilistic frameworks to account for the uncertainty and spatial variability of the material parameters.

In the 1990s, Finite Element Methods (FEM) and Finite Difference Methods (FDM) were introduced in the field of slope stability. These methods can be used together with LEM or alone. In the first case, seepage or stress-strain analyses are performed to determine the pore pressure or stress distribution in the slope to be used as input for LEM; in the second case, FS is calculated with the Strength Reduction Method (SRM), with the advantage that the failure surface is a result of the model and does not need to be defined a priori as in LEM. Advanced multi-phase formulations and constitutive models can be implemented in FEM and FDM. However, the results are limited to the onset of failure due to the numerical difficulties that arise when dealing with large deformations and consequent mesh tangling.

Several techniques have been proposed to simulate large displacements, e.g., Discrete Element Method (DEM) (Cundall and Strack, 1979), Arbitrary Lagrangian Eulerian (ALE) (Li and Liu, 2002), Coupled Eulerian–Lagrangian (CEL) (Qiu et al., 2011), Particle Finite Element Method (PFEM) (Idelsohn et al., 2003), Finite Element Method with Lagrangian Integration Points (FEMLIP) (Moresi et al., 2003), Smooth Particle Hydrodynamics (SPH) (Monaghan, 2012), Material Point Method (MPM) (Sulsky et al., 1994), etc. These methods can simulate the post-failure behaviour of the landslide, which is of great interest in

* Corresponding author.
E-mail address: francesca.ceccato@dicea.unipd.it (F. Ceccato).

https://doi.org/10.1016/j.enggeo.2024.107614
Received 5 December 2023; Received in revised form 22 May 2024; Accepted 27 June 2024
Available online 28 June 2024

evaluating the consequences of slope failure for risk assessment and mitigation. A detailed discussion on the differences and similarities of these methods exceeds the purpose of this paper, which focuses on MPM; the interested reader can find insightful comparisons between these numerical approaches in Augarde et al. (2021) and Soga et al. (2016).

The popularity of MPM has increased substantially in the last decade and the number of case studies analysed with this tool has increased sharply in recent years. This is probably due to the significant advancement of the numerical technique, its similarity to FEM, and the accessibility of open-source codes. MPM resembles FEM in many aspects (i.e., MPM can be perceived as an enriched FEM), making its understanding easier than other numerical techniques for people already familiar with FEM. In addition, most of the numerical techniques developed for FEM can be extended to MPM relatively easily, and the application of boundary conditions is more straightforward than other mesh-free methods owing to the presence of the background grid boundary. Table 1 reports a short list of freely available MPM codes that have been used for geotechnical applications; some of them are learning environments implemented in MatLab (AMPLE) or Python (MPM-Py), and other are advanced implementations in C++ or Fortran. This paper aims to discuss the current state of the art in modelling landslides with MPM, highlighting its advantages and disadvantages to serve as guidelines for future applications and encouraging the development of new solutions to current numerical challenges. A detailed discussion of the challenging mathematical and numerical aspects of the method itself and about the complexities and difficulties of simulating real landslides numerically exceeds the purpose of this work, which intends to provide a critical overview of the use of MPM for landslides and a practical guide for new applications in this topic. The paper provides a comprehensive review of MPM simulations of real landslide case histories discussing the main numerical features; literature on theoretical slope failures and laboratory-scale landslide simulations is not included.

The document is organized as follows. Section 2 provides a brief overview of MPM. Section 3 discusses its applicability to real cases reviewing the current literature with particular attention to the material constitutive models used in the simulations, the consideration of multi-phase interactions, and the numerical methodologies used to define the failure surface and triggering mechanisms. In Section 4, suggestions and best practices are given to serve as a guide for the future simulation of landslides using MPM. Limitations and future perspectives are discussed in Sections 5 and 6 to encourage the development of new solutions for current numerical challenges. Final conclusions are summarized in Section 7.

2. Material Point Method

MPM has been developed since the 1990s to simulate large displacements of history-dependent materials (Sulsky et al., 1995; Sulsky et al., 1994). It applies the principles of continuum mechanics, and the balance equations are discretised using a Eulerian grid (i.e., finite element grid) and Lagrangian points, called material points (MPs). The grid is typically fixed in space, and it is used to assemble and solve the field balance equations, typically, linear momentum balances. MPs are used to discretise the continuum mass; they store all the dynamic properties of the body, as well as material properties, mass, and loads. Large displacements are simulated by MPs moving through the grid that covers the whole domain, including empty spaces that are expected to be invaded during the calculation. This approach allows overcoming issues with element distortions typical of FEM. The computational cycle is illustrated in Fig. 1. At the beginning of each step, all the physical properties of the continuum are transferred from the MPs to the nodes of the computational grid by means of a mapping function (Fig. 1a). The governing equations (i.e., dynamic momentum balances) are solved for the primary unknown variables, i.e., the nodal accelerations (Fig. 1b). These nodal values are mapped back to the MPs by interpolating the grid results to update the acceleration, velocity and position of the MPs, as well as to compute strains and stresses (Fig. 1c, d). At that point, the nodal values are discarded since they are not required for the next step of the analysis, avoiding any element distortions.

Explicit time-integration schemes of MPM are suitable for short-duration dynamic problems and highly non-linear models. These approaches are computationally efficient but conditionally stable, namely their stability depends on the time increment of integration, which must be chosen carefully to avoid numerical instability. Several analytical expressions are available to evaluate the minimum time step required to ensure stability. For instance, the well-known Courant–Friedrichs–Lewy (CFL) condition that depends on element size, material stiffness, and density and is very accurate in single-phase calculations; however, in multi-phase hydromechanical frameworks, these expressions become more complex (Mieremet et al., 2015; Yerro, 2015; Yerro et al., 2022). Implicit schemes allow larger time increments that are convenient when simulating low-strain rates and quasi-static problems. They can provide an unconditionally stable solution but require the definition of a convergence criterion, allowing the iterative analysis to continue or not, depending on the accuracy of the results at the end of each step. As a result, the computational cost of the single increment is significantly higher than the explicit schemes.

Standard MPM (Sulsky et al., 1995; Sulsky et al., 1994) uses linear basis functions and assumes the mass is concentrated at the MP location. This formulation suffers from numerical instabilities, known as the cell-crossing error, which develop when MPs move across different elements in the computational mesh. To minimize this source of numerical noise, different alternative schemes have been proposed involving several basis functions and MP domains, such as the Generalized Interpolation Method (GIMP) (Bardenhagen and Kober, 2004), the Dual Domani MPM (DDMPM) (Zhang et al., 2011), the Convected Particle Domain Interpolation (CPDI) (Sadeghirad et al., 2011), or by using B-Splines (e.g. Steffen et al., 2008; Stomakhin et al., 2014), among others.

Soil is a mixture of solid, liquid, and gas phases, and several MPM formulations have been proposed to simulate the multi-phase hydromechanical interactions, which can be schematically summarized in Table 2. The rows indicate the number of phases explicitly considered in the balance equations, e.g. one-phase means that the material is modelled as an equivalent continuum representing the mixture and two-phase means that the balance equations of two constituents (solid and liquid) are considered separately including their interactions. The columns indicate the number of sets of MPs used to discretize the continuum phases; e.g., single-point means that the MPs represent the mixture and move according to the displacement of the solid phase, and double-point means that separate sets of MPs are used for the solid and liquid phases, and they move according to the displacements of the corresponding phase.

The one-phase single-point formulation is based on the standard

Table 1
Short list of open-source codes implementing MPM formulations.

Name of the code	Link	Language
AMPLE	https://wmcoombs.github.io/download/	MATLAB
Anura3D	www.anura3d.com	Fortran
CB-Geo	https://github.com/cb-geo/mpm	C++
COMDYN-MPM3D	http://comdyn.hy.tsinghua.edu.cn/english/mpm3d	Fortran
CoSim-MPM in Kratos	https://kratosmultiphysics.github.io/Kratos/	C++
fMPMM-solver	https://bitbucket.org/ewyser/fmpmm-solver/src/master/	MATLAB
Karamelo	https://github.com/adevaucorbeil/karamelo	C++
MPM-GIMP	https://sourceforge.net/p/mpmgimp/home/Home/	C++
MPM-Py	https://github.com/fabricix/MPM-Py	Python
NairnMPM	https://github.com/nairnj/nairn-mpm-fea/tree/master/NairnMPM	C++
Uintah	www.uintah.utah.edu	C++

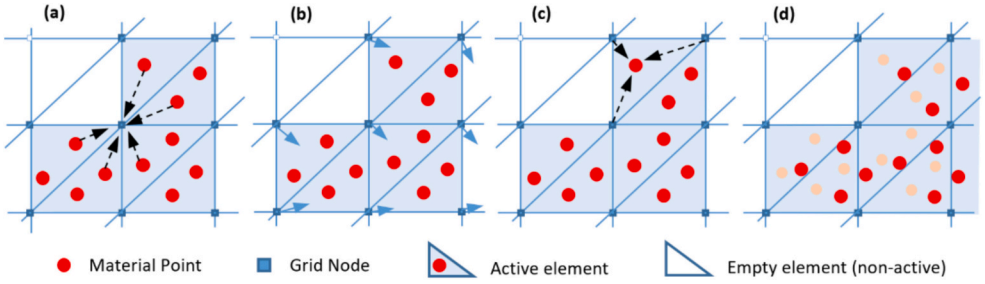

Fig. 1. Computation scheme of MPM: a) map information to the nodes, (b) solve the governing equations of motions at the nodes, (c) update MP quantities, (d) update MP position and housekeeping.

Table 2
Available MPM formulations.

		Number of phase MP set	
		Single-point	Double-point
Number of phase governing equations	One-phase		-
	Two-phase		
	Three-phase		

formulation (Sulsky et al., 1995; Sulsky et al., 1994) and can be adopted to model dry soil, pure liquid, as well as saturated soil in fully drained or undrained conditions where the presence of water can be considered in a simplified way. In drained conditions, a negligible excess pore pressure is generated, and this can be considered an input of the model. Under undrained conditions, the load rate is so fast that there is a significant generation of excess pore pressure but negligible relative movement between solid and liquid phases; therefore, pore pressure dissipation can be neglected.

The generation and dissipation of excess pore pressure are no longer negligible in saturated soil under partially drained conditions for which the fully coupled two-phase formulation is necessary (e.g. Alonso, 2021; Bandara and Soga, 2015; Jassim et al., 2013; Zhao et al., 2019). Partially saturated materials can be modelled with the fully coupled three-phase single-point formulation (Yerro et al., 2015) or by using simplified approaches that neglect the momentum and mass balance equations of the gas (see, e.g., Wang et al., 2016; Lei et al., 2020; Ceccato et al., 2023). A review of unsaturated MPM formulations is provided in Yerro et al. (2022). All these multi-phase formulations rely on single-point approaches, in which all the phases (e.g., solid skeleton, water, and eventually air) are represented by a unique set of MPs; the MPs move together with the solid motion (Lagrangian description), while the fluids are described using a Eulerian framework. This representation of the multi-phase media is convenient for many geotechnical applications, but it does not account for the physical separation between free water and solid skeleton required to represent, for instance, the impact of a landslide on a water reservoir. To overcome this limitation, two-phase double-point MPM formulations have been proposed (e.g. Abe et al., 2013; Bandara and Soga, 2015; Du et al., 2021; Liu et al., 2017; Martinelli, 2016) in which the soil skeleton and water phase are represented by different sets of MPs, denoted as solid MPs (SMPs) and liquid MPs (LMPs). Each set of MPs carries the information and provides a Lagrangian description of the corresponding phase. This framework comprises three potential subdomains, including saturated porous media (elements with both SMPs and LMPs), dry porous media (elements with only SMPs), and free water (elements with only LMPs). More recently, this same approach has been extended to include hydro-mechanical interactions resulting from partially saturated conditions (Feng et al., 2021a; Zhan et al., 2023); in these approaches, the information of the air phase (e.g., degree of saturation) is typically carried by the LMPs, while gas density and pressures are neglected.

3. Simulating real cases of landslides with MPM

MPM has been applied to a great number of real case studies; this section revises the existing literature to discuss the main numerical features used to capture the evolution of the landslide. In particular, we will focus on the type of material and constitutive models used, the relevance of soil-water interaction, the failure surface and sliding planes, and finally the triggering mechanisms used in the simulations. Simulations of experimental laboratory-scale slope failures are not considered here, nor parametric studies on theoretical slopes despite their relevance towards MPM validation. This is because we intend to focus on the potentialities and challenges of MPM for practical application to real cases. Snow avalanches are also not included (e.g. Gaume and Puzrin, 2021; Li et al., 2021a), although these phenomena have some similarity with landslides.

Tables A1 and A2 in Appendix A provide a list of papers that use MPM to simulate real landslides and summarise the salient characteristics of the considered case study and the simulation strategy. General observations from the literature review are as follows. All cases simulated with MPM so far have concerned rapid landslides. The reasons may be related to (i) the high interest of researchers in these hazardous phenomena and (ii) their suitability to be effectively simulated with MPM. In all the papers, dynamic explicit formulations are used, which are well suited for fast dynamic processes but inefficient for slow-moving landslides, although these can be, in principle, simulated. Although implicit MPM formulations have been developed since the beginning of the century (Guilkey and Weiss, 2001, 2003), to the authors' knowledge, there is only one application to a real case, i.e. Yamaguchi et al. (2023), where the implicit formulation is used only for the pre-failure stage (quasi-static conditions) and the dynamic explicit formulation is used for the post-failure stage. A few numerical model cases showed the potentiality of the implicit MPM for slope collapse; see, e.g. González Acosta et al. (2021a,b), Iaconeta et al. (2017), but a real case study has never been investigated yet using such integration schemes.

It is evident that the number of real cases investigated with MPM has increased substantially in the last few years (Fig. 2). The first attempts to use MPM in real cases adopted significant simplifications, e.g. simplified geometry and stratigraphy, simple constitutive models, oversimplified triggering mechanisms, and multi-phase simulations were disregarded, but in a few years the level of complexity increased considerably, being now able to simulate more realistically the complexity of real cases. Most of the published case studies are modelled in 2D for simplicity and to reduce computational cost. Full 3D simulations may require high computational effort; thus, computationally efficient algorithms are necessary.

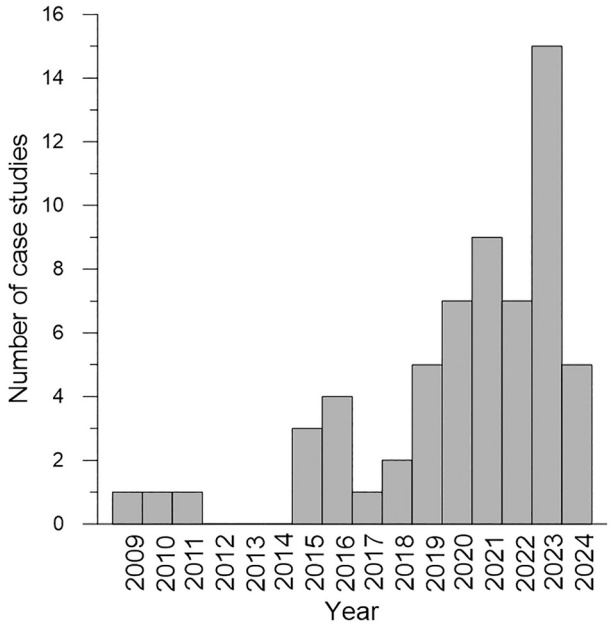

Fig. 2. Number of case studies published per year (updated May 2024).

Fig. 3 shows the software employed in these studies. Most researchers use open-source codes, but others developed *in-house* MPM formulations. Unfortunately, some of the papers do not mention this specific aspect and fall into the category *not stated*. Note that numerous authors developed and incorporated novel features into the open-source code to simulate the landslide under consideration that might not be available in the original source code at the link provided in Table 1.

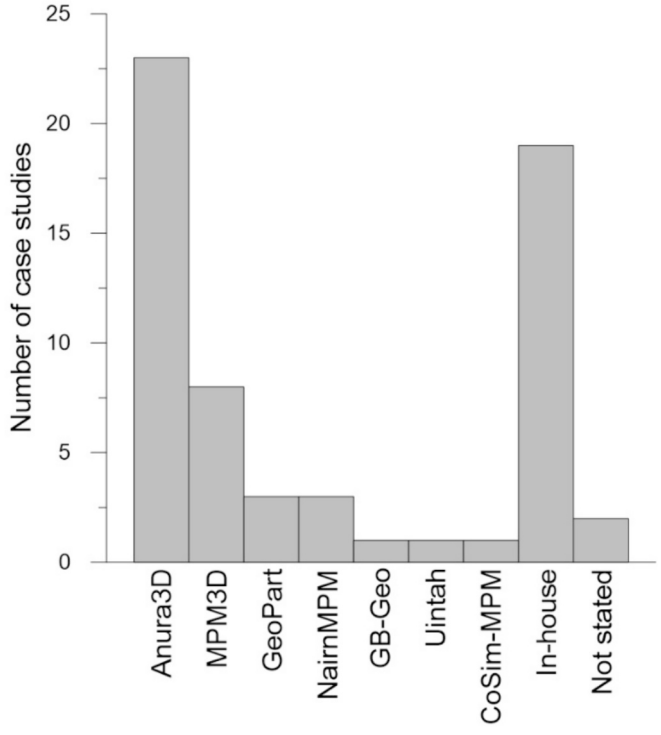

Fig. 3. Number of case studies analysed with different codes (updated May 2024).

3.1. Type of material and constitutive response

The considered case studies involved different types of material, such as hard and altered rock, coarse-grained and fine-grained soil, sensitive clay, tailings, and waste material. The selection of an appropriate constitutive model is a crucial aspect in any geotechnical model. When simulating landslides, key factors such as softening, strain-rate effects, temperature effects, liquefaction, and material destructuration, may play a relevant role in the runout and final shape of the slope. Very advanced history-dependent materials could theoretically be used in MPM, but large displacements and stress oscillations resulting from grid crossing errors, typical of MPM, may pose numerical challenges. Table 3 summarizes the constitutive models applied by the authors for different types of materials.

The landslide material is modelled in many cases with simple elastic-perfectly plastic models with Tresca, Von Mises, Mohr-Coulomb, or Drucker-Prager failure criteria. These models are always appropriate in preliminary analyses and can provide satisfactory results for materials with limited hardening/softening, such as loose and medium loose granular soils, normally consolidated clays, and fractured rocks. Since the post-failure phenomenon is governed by large deformations, operative shear strength parameters must be defined, which are usually close to the critical state or residual shear strength parameters.

Landslides in brittle materials such as sensitive or stiff clays or weathered rock require the use of strain-softening models to address failure initiation and long runout (e.g. Zabala and Alonso, 2011; Yerro et al., 2016a). Furthermore, strain-rate effects may be present at high shear rates, and shear resistance may increase (positive effect) or decrease (negative effect) depending on many factors (e.g., soil type, presence of water). This aspect can be incorporated in the constitutive model (Alvarado et al., 2019; Kohler and Puzrin, 2022; Pinyol et al., 2020; Tran et al., 2023; Tran and Sołowski, 2019), or in the frictional contact law (Li et al., 2021b) where the shear band is simulated with a contact algorithm.

Incorporating softening in constitutive models allows to better capture the transition from small to large strain soil behaviour and, therefore, long runout distances typical of many real cases. However, there are some numerical complications that should not be ignored. For example, the direct use of strain softening constitutive models entails the loss of objectivity of the results, in the sense that the strains tend to localize in a band that is only one element across, independently of the element size. Upon mesh refinement, strains tend to concentrate on a band of decreasing thickness, and less energy is dissipated in the failure process (i.e., localization problem). Clearly, this is physically unacceptable. In order to remedy this, different regularization techniques, well established in the finite element literature, can be extended to MPM. One of the simplest is the smear crack approach, which assumes that dissipation takes place in a band of only one element thickness and the parameters of the softening law are adjusted in such a way that the energy dissipated by the numerical shear band equals the work dissipated by the real shear band. In practical applications, this can be achieved calibrating the parameter of the constitutive model by simulating the results of laboratory tests with an MPM model applying the same mesh size of the discretization used for the landslide simulation (Soga et al., 2016). Sensitivity analyses should always be performed to investigate the effect of mesh size and constitutive parameters on the final shape of the failure surface and the runout, see e.g. Fern and Soga (2016), Troncone et al. (2023a), Yerro et al. (2016a).

The simulation of flow-like landslides is particularly challenging because the material undergoes phase transitions: it behaves as a solid during the inception and deposition phase (solid-like behaviour), i.e., stress chains exist between grains, and it behaves as a liquid during the propagation phase (liquid-like behaviour), i.e. the behaviour is governed by the collisions between grains. In addition, the (eventual) presence of the fluid phase is crucial. Establishing a unified phenomenological constitutive model to describe the multi-state behaviour of

Table 3
Summary of constitutive models used to simulate different types of materials with MPM.

Type of material	Constitutive response	Examples / references
Weathered Rock	Von Mises	Llano-Serna et al. (2015)
		Septian et al. (2017)
	Drucker-Prager	Liu et al. (2020)
		Zhang et al. (2023a)
	Drucker-Prager with strain softening	Li et al. (2021b)
		Zhao et al. (2021)
		Zhang et al. (2023b)
	Drucker-Prager + Rheological model	Xu et al. (2019)
	Nonlocal rheological model	Zhao et al. (2024)
	Mohr-Coulomb	Bhandari et al. (2016)
		Troncone et al. (2020)
		Ceccato et al. (2020)
		Cuomo et al. (2021)
		Nguyen et al. (2022)
		Yang et al. (2022)
		Yeh et al. (2022)
		Du et al. (2023)
	Mohr-Coulomb with strain softening	Yerro et al. (2016c)
		Pinyol et al. (2018)
		Feng et al. (2022)
		Yeh et al. (2022)
		Fernández et al. (2023)
	Mohr-Coulomb with strain softening and strain rate effect	Alvarado et al. (2019)
		Pinyol et al. (2020)
Coarse-grained soil (gravel, sand)	Mohr-Coulomb	Andersen and Andersen (2009; 2010)
		Macedo et al. (2024)
	Mohr-Coulomb with strain softening	Conte et al. (2019)
		Feng et al. (2021b)
	Drucker-Prager + Rheological model	Yamaguchi et al. (2023)
	Ta-Ger	Di Carluccio et al. (2024)
Fine-grained soil (silt, clay)	Von Mises	Llano-Serna et al. (2015)
	Tresca	Yerro et al. (2018)
	Mohr-Coulomb	Andersen and Andersen (2009; 2010)
		Ceccato et al. (2020)
		He et al. (2023)
	Mohr-Coulomb with strain softening	Zabala and Alonso (2011)
		Yerro et al. (2016c)
		Soga et al. (2016)
		Pinyol et al. (2018)
		Conte et al. (2019)
		Kularathna et al. (2021)
		Alonso (2021)
		Troncone et al. (2022)
		Macedo et al. (2024)
		Li et al. (2024)
	Mohr-Coulomb with strain softening and strain rate effect	Alvarado et al. (2019)
		Kohler and Puzrin (2022)
Sensitive clay	Mohr-Coulomb	Troncone et al. (2023a)
		Wu et al. (2023)
	Drucker-Prager with strain softening	Mei et al. (2020)
	Tresca	Troncone et al. (2023b)
	Tresca with strain softening	Liu et al. (2023)
		Troncone et al. (2023a)
	Tresca with strain softening and strain rate effect	Tran and Sołowski (2019)
Mixtures of sand, clay and silt	Tresca	Yerro et al. (2018)
	Tresca with strain softening	Conte et al. (2020)
	Mohr-Coulomb	Li et al. (2016)
		Zhu et al. (2022)
		He et al. (2023)
	Mohr-Coulomb with strain softening (suction dependent)	Yerro et al. (2015)
	Mohr-Coulomb + Rheological model	Müller and Vargas (2019)
	Mohr-Coulomb + Viscoplastic model in the shear band	Kohler et al. (2023)
	Drucker-Prager	Feng and Xu (2021)
		Du et al. (2021)
		Zhao et al. (2023)
	Drucker-Prager with strain softening	Shi et al. (2019)
		Ying et al. (2021)
		Tang et al. (2024)
Tailings	Tresca	Alonso (2021)
		Macedo et al. (2024)
	SANISAND	Lino Ramírez et al. (2023)

granular flows is difficult. Different alternatives can be found in the literature, which can be classified into fluid-based, soil-mechanics-based, and mixed theories. Fluid-based approaches use rheological models, soil-mechanics-based approaches use advanced constitutive models capable of incorporating material liquefaction, and mixed approaches combine these two ideas. Rheological models can be easily used in MPM and are preferred when the propagation phase is of main concern (Ceccato and Simonini, 2016; Dong et al., 2017). Advanced soil-mechanics-based approaches have been used when inception and consequent long flow distance is of interest, for example Di Carluccio et al. (2024), used the TaGer model, to simulate liquefaction in Valarties landslide and Lino Ramírez et al. (2023) used the SANISAND model for tailing dam failure. Xu et al. (2019) applied a mixed approach based on the Drucker-Prager yield criterion and the mu(I)-rehology to simulate the Hongshiyan landslide, while Müller and Vargas (2019) used the Mohr-Coulomb model for the prefailure stage and the Bingham model for the propagation stage of a debris flow in Santa Genoveva, Brazil.

Finally, the hard rocks that usually constitute the bedrock can be incorporated as a boundary condition or using linear elasticity. In addition, stiff structures eventually present in the slope (e.g. buildings, walls, or embedded piles) are well simulated with the linear elastic model or as rigid bodies.

3.2. *Relevance of multi-phase interactions*

Multi-phase interactions are certainly relevant in most cases; however, they can be accounted for in a simplified manner; indeed, the one-phase single-point formulation has been successfully used in those cases where fully drained or fully undrained behaviour of the material could be assumed. Undrained behaviour is appropriate for materials with low permeability, such as clay and rock, when the deformation rate is higher than the fluid dissipation rate. Total stress approache or effective stress approache may be used, with a prevalence of the first in the analysed cases reported in Table A2. Fully drained behaviour, i.e. excess pore pressure is set to zero, is commonly assumed for coarse-grained materials, e.g. debris, gravel, and sand. This type of material is sometimes used also for landslides triggered by changes in porewater pressures if the scope of the study is more orientated to the post-failure phase than to the triggering mechanisms. In these cases, the reduced shear strength due to the decrease of effective stress is simplified as a reduction of cohesion or friction angle (Andersen and Andersen, 2010; Feng and Xu, 2021; Nguyen et al., 2022; Yeh et al., 2022; Yu, 1993; Zhu et al., 2022).

Landslides induced by changes in pore pressure distributions in saturated and unsaturated conditions can be better captured with the two-phase single-point formulation for saturated and unsaturated soils, which can account for the coupled interaction between solid and fluid phases, eventually also considering the presence of gas in a simplified way. Fully coupled two-phase formulations allow a more realistic

simulation of the inception and propagation of rainfall-induced and seepage-induced landslides (Ceccato et al., 2020; Cuomo et al., 2021; Mei et al., 2020; Soga et al., 2016). The use of this approach is computationally more expensive, not only because the number of governing equations to be solved is doubled, but also because, in velocity-velocity formulations (true solid and liquid velocities are the primary unknown), applying the explicit Euler-Cromer scheme, the critical time step size reduces with the decrease of permeability (Mieremet et al., 2015; Yerro et al., 2022) and simulating materials of low permeability may require a very small time step size. Additional material properties to simulate the hydraulic coupling are necessary, which may be difficult to estimate, especially for unsaturated soils, i.e. soil-water retention curve, and hydraulic conductivity curve.

An even more advanced way of simulating unsaturated soils is the use of the three-phase single-point formulation, which explicitly considers the balance equations of the gas phase (Yerro et al., 2015). This approach is powerful, but the increase in complexity may be unnecessary in many applications where air pressure can be assumed constant and equal to atmospheric pressure.

One of the mechanisms invoked to explain the rapid acceleration of landslides is the heating of the shearing bands induced by the mechanical energy dissipated during sliding. To capture this effect, Pinyol et al. (2018) extended the two-phase formulation to non-isothermal conditions by including the energy balance equation, applying the assumption that the mechanical plastic work dissipates in heat. The shear band thickness, which is strongly influenced by the mesh size, has a significant effect on the dissipated energy and therefore on the landslide runout. To overcome this drawback, a numerical procedure has been developed in order to consider the real shear band thickness when performing numerical modelling of thermo-hydro-mechanical phenomena in landslides. The idea is to include a set of embedded shear bands in the material domain whenever the plastic deviatoric strain exceeds a reference value, and it is assumed that the strain computed at each material point will be assumed to be localised in an embedded shear band whose thickness will be given as an input parameter.

When the interaction between the sliding mass and free water is of interest, such as in submarine mass movements, landslide impacting on a water reservoir, or when the separation between solid and fluid phases during motion, as sometimes occurs in debris flows, is significant, the two-phase double-point formulation must be used. This formulation can also capture fluidization and sedimentation processes and account for variable soil concentration ratios. The application of the two-phase double-point formulation to real cases is still limited due to its complexity and computational cost. Furthermore, important simplifying assumptions, i.e. simplified geometry, simple material models, and triggering mechanism, were used to mimic landslide impacting in water reservoirs (Du et al., 2021, 2023).

Table 4 groups the MPM formulations used in several studies for various types of materials according to the drainage type.

Table 4
A summary of multi-phase interactions modelled with MPM.

Formulation	Material	Examples / references
One-phase single-point	Dry	Andersen and Andersen (2009, 2010) Li et al. (2016) Bhandari et al. (2016) Li et al. (2016, 2021) Septian et al. (2017) Conte et al. (2019) Xu et al. (2019) Zhao et al. (2021) Feng and Xu (2021) Yang et al. (2022) Feng et al. (2022) Yeh et al. (2022) Zhang et al. (2023a) Zhang et al. (2023b) Fernández et al. (2023) Du et al. (2023) Zhao et al. (2023)
	Saturated drained	Troncone et al. (2022) Kohler and Puzrin (2022) Zhu et al. (2022) Zhao et al. (2023) Kohler et al. (2023)
	Saturated undrained	Llano-Serna et al. (2015) Yerro et al. (2018) Shi et al. (2019) Tran and Sołowski (2019) Shi et al. (2020) Conte et al. (2020) Ying et al. (2021) Troncone et al. (2023a, 2023b) Liu et al. (2023)
Two-phase single-point	Saturated fully coupled	Zabala and Alonso (2011) Soga et al. (2016) Yerro et al. (2016b) Troncone et al. (2020) Müller and Vargas (2019) Conte et al. (2020) Mei et al. (2020) Pinyol et al. (2020) Kularathna et al. (2021) Alonso (2021) Nguyen et al. (2022) Lino Ramírez et al. (2023) Liu et al. (2023) Macedo et al. (2024) Li et al. (2024)
	Saturated fully coupled (with thermal effect)	Pinyol et al. (2018) Alvarado et al. (2019)
	Unsaturated fully coupled	Ceccato et al. (2020) Liu et al. (2020) Cuomo et al. (2021) Di Carluccio et al. (2024) He et al. (2023) Yamaguchi et al. (2023) Tang et al. (2024)
Three-phase single-point	Unsaturated fully coupled	Yerro et al. (2015)
Two-phase double-point	Saturated fully coupled	Du et al. (2021) Feng et al. (2021b) Du et al. (2023)

3.3. Failure surfaces and sliding base

The failure surface of a landslide refers to the surface along which the mass of soil, rock, or other material breaks away and starts to move downslope. This failure surface is a critical factor in understanding the mechanics and behaviour of landslides. Its shape and evolution depend on different factors such as geometrical and geological features of the slope, material behaviour, and triggering factors. In active landslides, the failure surface is already well defined in the slope, and the properties of the interface between stable and unstable material govern the post-failure dynamic. Similarly, in the propagation of flow-like landslides, terrain topography, and basal friction determine the kinematic of the flow. In first-time failures, the failure surface is initially absent and develops progressively within the slope during the inception phase. When weak layers are present, the plastic strain tends to localize at these locations. It should be noted that for active landslides, the evolution of their kinematic behaviour is the key point for risk management, while the calculation of FS is not informative, and thus large displacement analyses are necessary.

When the failure surface is well defined and known, the behaviour of the shear zone can be effectively simulated by applying a frictional contact law at the interface between sliding mass and stable ground by means of a contact algorithm. If the contact algorithm is not applied, MPM automatically enforces fully rough contact between interacting bodies or materials. With this approach, the number of key parameters governing the post-failure behaviour of the landslide is reduced to the

parameters of the contact law. The formulation originally proposed by Bardenhagen et al. (2001) and later improved in many studies (e.g. Ceccato et al., 2017; Hu and Chen, 2003; Ma et al., 2014; Nairn, 2019), has been applied in most of the papers mentioned in Table A2, and it has been further developed to account for shear rate effects (Li et al., 2021b). In addition, alternative contact algorithms have been proposed to improve computational cost and be able to simulate sliding along complex topographies efficiently (Du et al., 2023; Zhang et al., 2023a; Zhao et al., 2023).

In first-time failures, understanding the geometry and characteristics of the failure surface is crucial to predicting the potential extent and behaviour of a landslide. In these cases, the failure surface is a result of the simulation; therefore, the triggering mechanism should be carefully simulated. Weak layers can be included in the numerical model with MPs of appropriate constitutive behaviour, but it should be noticed that their simulated thickness is usually much larger than reality because very small mesh sizes increase the computational cost. Moreover, during large movement, elements containing different materials occur, thus causing an averaging effect during mapping of internal forces to the grid nodes.

An interesting advantage of MPM, compared to FEM and LEM, is that progressive failures, retrogressive landslides, and other cascading effects can be simulated. Indeed, since FEM and LEM are limited to small deformations or consider the undeformed configuration of the slope, the effect of the displaced mass on the stability of the upper part of the slope and the consequences of the downward movement of the landslide cannot be assessed.

3.4. Triggering mechanism

Real landslides may be triggered by many different factors, e.g. excavation, earthquakes, changes in water pressure and seepage, material degradation, or a combination of more than one of them, which can be simulated numerically with different strategies depending on the level of complexity of the model and the main goal of the study. Table 5 combines the prevalent triggering factor of the real landslide with the simulated triggering factor used by different authors.

When the main goal of the study is investigating the landslide post-failure kinematics, oversimplified numerical triggering mechanisms are often applied, such as

(i) release of the soil mass under gravity without prior generation of initial stresses in static conditions,
(ii) progressive increase of gravity or soil unit weight,
(iii) release of displacement constraints after initial stress generation,
(iv) sudden reduction of shear strength parameters.

Strategies (i)-(iii) are not representative of any physical process, while strategy (iv) can simulate material weathering or shear strength reduction due to a decrease of effective stresses when this is not explicitly simulated with multi-phase formulations. These approaches disregard the hydromechanical processes involved in the inception phase and assume that they have a negligible influence on the post-failure behaviour. This assumption is also common in hydrodynamic propagation models for flow-like landslides, and it is considered acceptable for these phenomena, but it is discouraged in other types of landslides.

Landslides induced by increasing porewater pressure in the slope simulated with multi-phase simulations can be triggered by:

(i) reducing soil cohesion,
(ii) changing the pore pressure at the MPs importing results calculated with other methods,
(iii) applying a pore pressure traction or infiltration boundary condition.

Table 5
Summary of landslides triggering factors simulated with MPM.

Real triggering factors	Simulated triggering factor	Examples / references
Construction method	Dam construction	Zabala and Alonso (2011)
	Reduction of shear strength	Alonso (2021)
	Reduction of shear strength and excavation	Macedo et al. (2024)
Excavation	Reduction of shear strength	Conte et al. (2019)
	Excavation	Troncone et al. (2022)
	Excavation	Tran and Sołowski (2019)
Toe erosion		Feng and Xu (2021)
	Reduction of shear strength	Liu et al. (2023)
		Troncone et al. (2023a, b)
		Li et al. (2016)
		Xu et al. (2019)
	Increase of gravity	Mei et al. (2020)
		Shi et al. (2020)
		Li et al. (2021b)
		Du et al. (2021)
	Reduction of shear strength	Du et al. (2023)
		Bhandari et al. (2016)
	Prescribed velocity-time history	Pinyol et al. (2020)
Earthquake		Fernández et al. (2023)
		Feng et al. (2021b)
	Prescribed traction-time history	Kohler and Puzrin (2022)
		Kohler et al. (2023)
	Equivalent nodal forces mapped from SEM calculation	Feng et al. (2022)
	Increase of soil unit weight	Andersen and Andersen (2009)
		Llano-Serna et al. (2015)
	Increase of gravity	Ying et al. (2021)
		Zhao et al. (2021)
		Zhao et al. (2024)
		Andersen and Andersen (2010)
		Yerro et al. (2018)
	Reduction of shear strength	Zhu et al. (2022)
		Yeh et al. (2022)
Rainfall		Troncone et al. (2023b)
	Release of initial constraints	Du et al. (2023)
		Zhao et al. (2023)
	Zero pressure at boundary	Yerro et al. (2015)
		Liu et al. (2020)
		Cuomo et al. (2021)
	Infiltration boundary condition	He et al. (2023)
		Yamaguchi et al. (2023)
		Tang et al. (2024)
Wetting of the toe	Increase of groundwater level (updating the pore pressure at MPs)	Pinyol et al. (2018)
Reservoir drawdown	Sudden change of pore pressure at MPs	Alvarado et al. (2019)
Increase of groundwater table	Increase of gravity	Conte et al. (2020)
		Shi et al. (2019)
	Reduction of shear strength	Nguyen et al. (2022)

(continued on next page)

Table 5 (*continued*)

Real triggering factors	Simulated triggering factor	Examples / references
Increase of pore water pressure (e.g. snowmelt, karstic spring)	Pressure boundary condition	Troncone et al. (2020) Soga et al. (2016) Ceccato et al. (2020) Kularathna et al. (2021) Lino Ramírez et al. (2023) Di Carluccio et al. (2024) Li et al. (2024)

Strategy (i) is used to simulate the decrease of apparent cohesion due to suction in unsaturated soils when partial saturation is not explicitly accounted for in the formulation, but it can also represent material degradation. Strategy (ii) requires the simulation of the hydraulic process up to failure with another software (e.g., FEM, FDM) and a tool to import the corresponding results in MPM. Here, only post-failure is investigated with MPM, which can be an efficient solution, especially for slow seepage and infiltration processes. It should be ensured that the two models apply similar hydromechanical material properties and boundary conditions. Strategy (iii) simulates directly the hydraulic load causing failure and the corresponding hydromechanical soil response; it allows the simulation of pre- and post-failure behaviour, but it can be computationally expensive for slow infiltration processes.

Instabilities induced by construction or excavation/erosion are simulated with specific construction/excavation tools available in the software or by changing the material properties of the excavated material. It should be noted that, at present, available MPM codes are not as well developed as FEM/FDM software tools for the reproduction of different construction phases. In the pioneering paper by Zabala and Alonso (2011) the progressive failure of a dam foundation is simulated including the dam construction by layers. However, the paper focuses on the evolution of shear bands, while the post-failure large displacements were not investigated. As far as the authors are aware, the only other contribution to the development of this feature for MPM is the recent work by Aviles et al. (2024).

When the simulation of earthquake-induced landslides is of interest, special boundary conditions are necessary. In particular, two approaches can be used to apply the seismic motion: (i) application of kinematic time-history directly from processed ground motion recordings (i.e. acceleration, velocity), (ii) application of equivalent traction history (i.e. a velocity recording is transformed into normal and shear stress). Feng et al. (2022) coupled MPM with the Spectral Element Method (SEM). At a regional scale, SEM is used to model elastic wave propagation from a seismic source to a local site with complex topography, and the results are used as BC for the MPM model of the slope. Special procedures are necessary to ensure the compatibility between the methods. These types of dynamic simulations are complex and require accurate time integration schemes that can dissipate high frequency numerical noise and special treatment of the boundary conditions (e.g. periodic, free field, or absorbing boundaries) to capture the propagation, amplification, and attenuation of the seismic waves in the computational domain in a realistic manner mimicking site conditions. The development of these features and strategies in the MPM framework is currently ongoing, and the validation of site response is crucial to accurately capture the loading time history at different locations, see e.g. Alsardi and Yerro (2023). The simulations of real earthquake-triggered landslides are summarized in Table A2. These represent pioneering works and apply only some of these features. The use of MPM to evaluate the consequences of seismic landslides is expected to grow, considering the limitations of current permanent displacement predictive methods to evaluate the performance of liquefiable soils in complex stratigraphic conditions.

4. Best practices in modelling landslides with MPM

The previous section presented a review of real case histories investigated and numerically modelled with MPM showing that the method can be a valuable support to improve the understanding of the evolution of landslides from inception to deposition. This tool will play a significant role in future developments of landslide modelling, and it may be used also in standard engineering practice. The spread of knowledge and guidance in the application of MPM can facilitate the use of this numerical method in practise. For this purpose, this section attempts to formulate a list of best practices for the simulation of landslides with MPM.

MPM simulations are advanced numerical simulations; this means that all the steps normally taken to build a numerical model must be applied. The reader can refer to the literature on numerical modelling in geomechanics for further details, e.g. Fern et al. (2019), Lambe (1973), Wood (2004), Zienkiewicz et al. (1999a). In addition, the level of complexity should be progressively increased and it is always suggested to perform preliminary stability analyses with LEM, FEM, or FDM. These methods provide useful insights towards understanding the failure mechanisms, and the key factors controlling the pre-failure and failure stages can be efficiently investigated quantitatively.

In geomechanics, the estimation of material parameters and ground conditions is inherently uncertain due to difficulties in subsurface exploration and natural variability of the materials. For landslides, this is even more complicated because the pre-failure conditions are usually unknown and, after the event, they can only be hypothesized. Even very advanced numerical simulations entail a certain level of simplification and require a number of assumptions that should be taken in due count to assess their effect on the final results. This can be done by applying engineering judgment, performing parametric studies, and considering different simulation scenarios.

Initial conditions are relevant in the development of the failure mechanism; therefore, an appropriate initialization procedure should be applied. The K0-procedure, in which the vertical stress is proportional to the depth of the point and the horizontal stress is a pre-defined fraction of it, is not recommended for slopes, and the gravity loading procedure should be preferred. Note that linear elastic model or high shear strength parameters are necessary in this phase to avoid unrealistic yielding in the slope due to dynamic effects when applying gravity. When performing gravity loading with a dynamic formulation, it is necessary to verify the convergence to quasi-static equilibrium. This can be done by checking that the kinetic error ε_{KE} (Eq. (1)), and the unbalanced force error ε_F (Eq. (2)), are below a certain threshold tol_{KE} and tol_F, typically of the order 10^{-4}:

$$\varepsilon_{KE} = \frac{KE}{W_{ext}} < tol_{KE} \tag{1}$$

$$\varepsilon_F = \frac{|F_{ext} - F_{int}|}{|F_{ext}|} < tol_F \tag{2}$$

In Eqs. (1) and (2), KE si the kinetic energy, W_{ext} is the work of external forces (gravity), $|F_{ext} - F_{int}|$ is the norm of unbalanced forces and $|F_{ext}|$ is the norm of external forces (gravity).

The quasi-static gravity loading phase may require long simulation times; to accelerate convergence, the local damping early introduced in Coetzee (2005) can be applied with relatively high local damping factors, e.g. 0.7. For multi-phase formulations, local damping applied to the fluid phase may delay the dissipation of excess pore pressure (Ceccato, 2014; Yerro et al., 2016a) and should be used cautiously. Moreover, in many cases, the initial conditions are characterized by stationary seepage; thus, Eqs. (1) and (2) cannot be applied to the liquid phase. Local damping can significantly alter the failure mechanism and reduce the runout; therefore, during the inception and propagation of the

landslide, it should not be used. Very small values of damping factor, e.g. 0.01–0.05, may be applied to stabilize the simulation, upon verification of its minimal effect on the results, or to include artificially some form of energy dissipation not accounted for by the constitutive model.

Mass scaling is a procedure typically used in dynamic explicit formulation to increase the critical time step size and reduce the computational time (Ceccato and Simonini, 2019), but it should not be used in the simulation of landslides because it artificially increases the mass of the system, thus altering its dynamical behaviour and leading to shorter runout.

Another challenge is to discretize the given problem and solve it with MPM, obtaining a reasonably accurate result in an acceptable time. It is always recommended to check the spatial convergence of the solution by solving the same problem with a finer grid (while maintaining the same number of MPs per grid cell) and with an increased number of MPs per cell (while maintaining the same grid) and comparing the results. Further refinement should be conducted if there is a difference between the two final results that exceeds the desired level of accuracy. In most cases, the accuracy of the results and computational cost are more affected by the grid size than by the number of MPs. Note that the original MPM formulation (Sulsky et al., 1994) suffers from grid crossing error, i.e. numerical error occurring when MPs move from one element to another; thus, increasing the number of MPs may worsen this issue. Although several variants of MPM, such as GIMP, CPDI, DDMP, and BSMPM, have been introduced to reduce this problem, it cannot be fully eliminated.

During a landslide propagation phase, MPs move through the computational mesh, and eventually one element may remain empty until the next MP goes into it. This fact creates unrealistic small holes within the continuum and produces discontinuities of the strain and stress fields, potentially leading to the numerical instability of the simulation. The frequency of the problem depends on the spatial discretisation and worsens when the initial number of MPs per element is small, or the computational mesh is very fine. It can be mitigated by a careful discretization, ensuring that there is a sufficient number of MPs to minimize the occurrence of empty elements during their motion across different elements. Another solution is to add virtual materials points that are used as integration points in the empty elements (Yerro, 2015). The mass of virtual points should be negligible to keep the total mass of the system approximately constant.

In principle, the influence of the time-step size should also be checked. However, the errors arising from time steps are typically much smaller than those related to discretization, as long as the time step is kept well below the Courant-Friedrichs-Lewy stability condition.

5. Limitations and challenges

Despite the great developments of MPM in recent years, several limitations and challenges still need to be addressed in the future to improve the simulation of landslides.

One of the most difficult and discussed topics is the hydromechanical behaviour of the materials constituting the landslide. This is clearly not only a limitation of MPM, as constitutive modelling is a key issue in all geomechanical problems, but for landslides, it may become very complicated when factors such as strain rate, material softening, and temperature are relevant and when the material experiences a transition between solid-like and fluid-like behaviour. Advanced constitutive models have been proposed in the literature, but their applicability to real cases is hampered by numerical difficulties associated with stress oscillations due to grid crossing, and difficulties with the calibration of the parameters. Significant improvements have been made in the past years to mitigate stress oscillations and improve accuracy, see Sołowski et al. (2021) for an overview, which may facilitate the use of these models in the future. Parameter calibration is usually based on laboratory tests at small displacements and in quasi-static conditions (for mechanic-based models) and, therefore, may be questionable for the real case. Moreover, strain-softening models suffer from mesh dependency, which should be accounted for during calibration, as mentioned in Section 3.1.

The minimization of unrealistic stress oscillations is also essential for the application of MPM on the study of earthquake-triggered landslides to accurately capture the slope performance and, for instance, the extension of liquefaction in the soil mass. These models require (i) the use of techniques to reduce numerical cell crossing, (ii) the implementation of time integration schemes that can capture site response (e.g., avoid Euler-Cromer), and (iii) the consideration of adequate boundary conditions that can mimic site conditions and avoid unrealistic wave reflections and tractions in the soil. Much knowledge can be transferred from existing mesh-based numerical technics (FEM, FDM) with few variations (e.g. MP relocation algorithms or moving mesh technique); however, the majority of current MPM codes do not include these features yet.

Another relevant constitutive feature of rock and stiff clays is the anisotropy of the material. Although it could be easily included in small deformation problems, it poses a significant challenge at large displacement when the material is remoulded, and it has never been considered in MPM landslide simulation up to now.

In the context of actual geological structures, the enormous difference of scales between the thickness of fissures, joints, and very thin layers and the size of the landslide complicates their simulation due to the need for very small mesh elements, which may excessively increase the computational cost. Furthermore, with the movement of MPs through the grid, elements can contain MPs of different materials; thus, a smearing effect occurs during the mapping of properties from MPs to nodes. Similarly, the real thickness of a shear band cannot be naturally simulated in MPM, and a special treatment is necessary. In the attempts to resolve the evolution of shear bands and cracks more accurately, several enhancements of the MPM, including nonlocal models (Burghardt et al., 2012), multiscale approaches (Liang and Zhao, 2019), phase-field method (Kakouris and Triantafyllou, 2017), and local enrichment of shape functions (Liang et al., 2022; Liang et al., 2017) have recently been proposed and appear promising for application to landslides.

One of the main limitations of MPM is its computational cost, which remains higher than FEM, but is usually lower than DEM and SPH. Generally, the computational cost of a real landslide simulation is high, and therefore an efficient numerical code is necessary. At present, most of the existing MPM codes for geomechanical applications are based on central processing unit (CPU), and parallel computation tools, such as OPEN-MP and MPI, are applied in some algorithms (e.g. MPM3D, CB-Geo, Anura3D). Some MPM algorithms are based on the graphic processing unit (GPU) framework, which offers higher computational speed (Feng and Xu, 2021; Zhang et al., 2023a; Zhao et al., 2019). The increase in computational power will certainly favour the use of the method in the future, but the implementation of efficient solvers is always necessary.

To simulate real landslides in an acceptable time, different assumptions and numerical tricks have been adopted to reduce the computational cost. Examples are the simplification of the triggering factors (to avoid the simulation of long triggering processes) and the adjustment of the material parameters such as elastic moduli and permeability (to increase the critical time step size and reduce the duration of seepage processes).

Despite the significant advancement of the numerical methodology in recent decades, no single MPM code incorporates all recent developments because the community is fragmented. This means that each MPM software has its strengths and weaknesses that should be accounted for by new users willing to use the method for their research or practical applications. Furthermore, most of the available open-source software does not come equipped with user-friendly pre- and post-processors and tutorial manuals, such as most of the commercial FEM software, but part of the MPM research community is paying

significant effort in making these codes easier to be used by students and practitioners.

6. Future perspectives

The Material Point Method has greatly matured since the first publication of Sulsky et al. (1994) and proved to be well applicable to landslide simulation, even considering the complexity of real cases. At present, it is only applied for academic and research purposes, but in the future, it can certainly become a standard tool of engineering geology practice. There is perhaps a need for more user-friendly software accompanied by a dissemination of knowledge and an increase of awareness of the capabilities of the method at the level of engineering geology practitioners. To this end, a sequential use of MPM with other methods used in the state-of-the-practice, e.g. FEM, LEM, is probably one of the best options. The idea is to apply each method to the part of the simulation for which it is optimal. For example, Alvarado et al. (2019), Ceccato et al. (2023), Lu et al. (2023) used FEM to calculate the pore pressure and stress distribution in the slope before failure and used the results to initialize the MPM simulations for the post-failure stage. Note that in Ceccato et al. (2023), the pre-failure phase is simulated with well-established commercial codes, and therefore, the subsequent use of MPM for the post-failure analyses may appear relatively easy to engineers and geologists.

Coupling MPM with other advanced numerical techniques such as molecular dynamics (MD) (Chen et al., 2011), FEM (Chen et al., 2015), DEM (Liang and Zhao, 2019), SEM (Feng et al., 2022), to perform multiscale and multiphysics simulations is a promising research topic, which will contribute to advance the current understanding of landslide processes; however, at present, it appears still far to be introduced into standard-level practical applications.

Random fields have been introduced in MPM to account for the spatial variability of soil properties and investigate its consequence on the post-failure behaviour, see e.g. Qu et al. (2021), Remmerswaal et al. (2021), Wang et al. (2016). So far, this technique has only been illustrated with simplified model cases, but it can be extended to more realistic scenarios for quantitative risk assessment. The level of complexity of these analyses and the required computational cost are significant. However, the tool clearly offers an interesting opportunity given the increasing interest in quantitative landslide risk assessment.

Slow-moving and creeping landslides have never been simulated with MPM so far. This is due to the computational cost of explicit simulations, which may probably be circumvented by using implicit schemes that allow larger time step sizes. However, the computational cost of the implicit time increment is much larger, and thus the computational convenience is not guaranteed. As far as the authors are aware, there are no comparisons of explicit and implicit methods in terms of both accuracy and computational efficiency for problems involving non-linear materials and large displacements, as typically used in geomechanics. More research is encouraged on this topic.

Modelling reinforcements (piles, anchors, geogrids, etc.) is often of interest for practical applications. Still, at present, they are simulated as inclusions of stiff materials because the implementation of structural elements typical of FEM, such as beam and truss, is difficult to extend to large deformation MPM simulations. This line of research could further increase the applicability of the method to real cases and further investigate the reliability of remediation measures.

Despite the advances of the last decades, additional work is needed to improve the accuracy and robustness of the method, especially when complex geometries and non-linear constitutive models are used. This is important to increase the reliability of the results and the confidence of users in the methodology.

Finally, more research on constitutive modelling is required to accurately simulate the entire landslide process, from initiation to deposition. This observation is clearly not specific to MPM and can obviously be extended to any modelling tool.

7. Conclusions

In the last 15 years, the Material Point Method has been demonstrated to be capable of simulating the post-failure behaviour of a number of real landslides. The numerical features of the simulations addressing this problem have been analysed, with emphasis on constitutive modelling of the material, multi-phase interactions, numerical simulation of sliding surfaces, and triggering factors. The level of complexity has increased sharply in the last 15 years, and the available codes have been enriched with several tools to capture the essential aspects of the phenomenon. Not all the latest computational developments and innovative features of the method have been applied to real cases yet because further validations are necessary, but in the near future they will offer new opportunities to improve the simulation of slopes.

Suggestions for the use of MPM have been provided for practical cases, with the aim of being a useful guide for new studies. Potentialities, limitations, and challenges of the method have been discussed. Note that despite this paper focus on MPM, many observations are also valid for other methods, e.g. PFEM, FEMLIP, and SPH, which may have some similarities with MPM.

Despite the higher complexity and computational cost of MPM simulations, compared to traditional LEM and FEM, the ability to model progressive failure, long runout distances, and other cascading effects is fundamental to advance the current understanding of landslides and improve risk assessment and management. We believe that the use of MPM will increase further in the future, possibly becoming a standard practice for landslide modelling, as occurred for LEM and FEM in the past.

CRediT authorship contribution statement

Francesca Ceccato: Writing – review & editing, Writing – original draft, Software, Resources, Methodology, Conceptualization. **Alba Yerro:** Writing – review & editing, Writing – original draft, Software, Conceptualization. **Gaia Di Carluccio:** Writing – review & editing, Writing – original draft, Investigation.

Declaration of competing interest

The authors declare that they have no known competing financial interests or personal relationships that could have appeared to influence the work reported in this paper.

Data availability

Data will be made available on request.

Acknowledgements

The authors aknowledge the project PDC2022-133222-I00 funded by MCIN/AEI/10.13039/501100011033 and by “European Union Next Generation EU/PRTR", and the project BIRD181859 funded by the University of Padua.

Appendix A

This appendix summarizes in Table A1 the main characteristics of the real cases analysed with MPM in research papers (name of the landslide, year, location, materials and triggering factors), and in Table A2 the key numerical features of the simulations (multiphase formulation, name of the code, constitutive models, numerical triggering factor, use of contact algorithm, 2D or 3D dimension)

Table A1
List of real landslides simulated with MPM in research papers.

Citation	Year of publication	Case study	Country	Year of landslide	Materials	**Triggering factors**
(Andersen, 2009)	2009	Lønstrup	Denmark	2008	Clay and sand	heavy rainfall
(Andersen & Andersen, 2010)	2010	Lønstrup	Denmark	2008	Clay and sand	heavy rainfall
(Zabala & Alonso, 2011)	2011	Aznalcollar Dam	Spain	1998	Clay	construction method
(Llano-Serna et al., 2015)	2015	Vajont	Italy	1963	Rock and clay	wetting of the toe
(Llano-Serna et al., 2015)	2015	Tokai-Hokuriku expressway	Japan	1999	not stated	heavy rain
(Yerro et al., 2015)	2015	Collapse of Girona road embankments	Spain	2010	mixture of sand and clay	rainfall
(Soga et al., 2016)	2016	Selborne experiment	UK	1989	Clay	increase of pore pressure by surcharge wells
(Yerro et al., 2016b)	2016	Vajont	Italy	1963	Rock and clay	wetting of the toe
(X. Li et al., 2016)	2016	Wangjiayan landslide	China	2008	Gravel, silt, and clay	earthquake
(Bhandari et al., 2016)	2016	Chiu-fen-erh-shan landslide	China	1999	Rock	earthquake
(Septian et al., 2017)	2017	Bingham Canyon mine	USA	2013	Rock	unclear
(Yerro et al., 2018)	2018	Oso landslide	USA	2014	Sand, clay and silt	prolonged intense rainfall
(Pinyol et al., 2018)	2018	Vajont	Italy	1963	Rock and clay	wetting of the toe
(Conte et al., 2019)	2019	Senise	Italy	1986	Sand and clay	deep excavation
(Tran & Sołowski, 2019)	2019	Sainte-Monique, Quebec	Canada	1994	Sensitive clay	toe erosion
(B. Shi et al., 2019)	2019	Shenzhen landfill landslide	China	2015	Waste, rock, sandy clay	increase of water table (rainfall)
(Xu et al., 2019)	2019	Hongshiyan landslide	China	2014	Rock fragments	earthquake
(Alvarado et al., 2019)	2019	Canelles	Spain	2006	Rock and clay	rapid drawdown
(Müller & Vargas, 2019)	2019	Santa Genoveva debris flow	Brazil	1988	Colluvium, rock	heavy rain + boulder impact
(Troncone et al., 2020)	2020	Cook Lake	USA	1997	Rock	increase of groundwater table (prolonged rainfall)
(Pinyol et al., 2020)	2020	Tsaoling	Taiwan	1999	Rock	earthquake
(Conte et al., 2020)	2020	Maierato	Italy	2010	Silty sand and clayey silt, rock	heavy rainfall, increase of groundwater water level
(Mei et al., 2020)	2020	Storegga Slide	Norway	8200 years ago	Sensitive clays	earthquake, gas hydrate decomposition
(J. J. Shi et al., 2020)	2020	Submarine escarpment failure in the Southern Mediterranean	Not stated	Not stated	Not stated	earthquake
(Ceccato et al., 2020)	2020	San Vigilio di Marebbe	Italy	2008	Debris, rock, clayey silt	snowmelt, pipe damage, increase of groundwater table
(X. Liu et al., 2020)	2020	Fei Tsui Road landslide	Hong Kong	1995	Rock	heavy rainfall
(Cuomo et al., 2021)	2021	Fei Tsui Road landslide	Hong Kong	1996	Rock	heavy rainfall
(Li et al., 2021)	2021	Daguangbao	China	2008	Rock	earthquake
(Ying et al., 2021)	2021	Xinlu Village	China	2016	Rock, silty clay, breccia	heavy rainfall
(Du et al., 2021)	2021	Lituya Bay landslide	USA	1958	Moraine deposits	earthquake
(K. Feng et al., 2021)	2021	Lower San Fernando dam	USA	1971	Zoned earth-filled embankment	earthquake
(Zhao et al., 2021)	2021	Xinmo village	China	2017	Rock	prolonged low-intensity rainfall
(Z. K. Feng & Xu, 2021)	2021	Dongmiaojia landslide	China	Not stated	Soil-rock mixture	river erosion, weathering and saturation of weak layers
(Kularathna et al., 2021)	2021	Selborne	UK	1989	Clay	increase of pore pressure by surcharge wells
(Alonso, 2021)	2021	Aznalcollar Dam	Spain	1998	Clay	construction method, tailing liquefaction

(*continued on next page*)

Table A1 (*continued*)

Citation	Year of publication	Case study	Country	Year of landslide	Materials	**Triggering factors**
(Troncone et al., 2022)	2022	Caloveto	Italy	2014	Clay, sandy silt	excavation
(Yang et al., 2022)	2022	Hongshiyan landslide	China	2014	Rock	earthquake
(Nguyen et al., 2022)	2022	Jintou Mountain	Taiwan	2008	Rock	rainfall infiltration, increase of groundwater level
(Kohler & Puzrin, 2022)	2022	La Sorbella landslide	Italy	not occurred yet, it is a stability analysis	Clay and silt	earthquake
(Zhu et al., 2022)	2022	Hidaka mountains	Japan	2003	residual soil, rock	rainfall
(K. Feng et al., 2022)	2022	Hongshiyan landslide	China	2014	Rock	earthquake
(Yeh et al., 2022)	2022	Translational landslide at kilometer marker 3.1K of the Freeway No. 3	Taiwan	2010	Rock	weathering, rainfall infiltration, increase of groundwater level, rupture od ground anchors
(Troncone et al., 2023b)	2023	Saint-Jude	Canada	2010	Sensitive clays	river erosion and increase of pore water pressures
(He et al., 2023)	2023	Boli landslide	China	2018	Silty clay, argillaceous gravels	heavy prolonged rainfall
(Zhang et al., 2023a)	2023	Baige landslide	China	2018	Rock	heavy rain
(Du et al., 2023)	2023	Erhuang Village landslide	China	2011	Rock	rainfall
(Z. Q. Liu et al., 2023)	2023	Ask in Gjerdrum	Norway	2020	Sensitive clays	toe erosion
(Lino Ramírez et al., 2023)	2023	Sullivan	Canada	1991	Tailings	increase of pore water pressure
(Zhao et al., 2023)	2023	Yanyuan landslide	China	2018	Sandy clay with sandstone debris, rock	rainfall
(Zhang et al., 2023b).	2023	Jiweishan rockslide	China	2009	Rock	evolution of long-term creep
(Yamaguchi et al., 2023)	2023	Ashikita town, Kumamoto	Japan	2020	Sandy gravel	rainfall
(Kohler et al., 2023)	2023	Marsc landslide	Switzland	Since 1990	Sedimentary rocks, silty sand gravel, cobbles and boulders	earthquake
(Troncone et al., 2023a)	2023	Saint-Monique landslide	Canada	1994	Sensitive clay, silty clay	toe erosion
(Troncone et al., 2023a)	2023	Baastad landslide	Norway	1974	Marine silty clay, sensitive clay	rainfall and agricultural works
(Wu et al., 2023)	2023	Yanlian landslide	China	2010	Malan loess	increase of groundwater level
(Du et al., 2023)	2023	Xinhua Village landslide	China	2022	Granite, weathered rock, debris, gravel	earthquake
(Fernández et al., 2023)	2023	Daguangbao landslide	China	2008	Limestone, mudstone and dolomite rocks	earthquake
(Macedo et al., 2024)	2024	Cadia dam failure	Australia	2018	Mine tailings, clay, rockfill	construction method, excavation
(Di Carluccio et al., 2024)	2024	Valarties, Val d'Aran	Spain	2018	Silty sand	karstic spring after a rainfall period
(Tang et al., 2024)	2024	Yanyuan landslide	China	2018	Silty clay with gravel	rainfall
(Y. Li et al., 2024)	2024	Selborne experiment	UK	1989	Clay	increase of pore pressure by surcharge wells
(Zhao et al., 2024)	2024	Nayong rock avalanche	China	2017	Rock	mine tunnel collapse, rainfall

Table A2
Numerical features of the MPM simulation of real landslides in research papers. Acronyms of the shape of failure surface: MC = Mohr-Coulomb, VM = Von Mises, T = Tresca, DP=Drucker-Prager; SS = strain softening effects are included; SR = Strain rate effects are included; R = rheological model for fluidized conditions.

Citation	Formulation	Code	Constitutive models	Simulated triggering factors	**Contact algorithm?**	**2D/ 3D**
(Andersen and Andersen 2009)	one-phase single-point	in-house	MC	increase of soil density	yes (Bardenhagen)	2D
(Andersen and Andersen, 2010)	one-phase single-point	in-house	MC	reduction of shear strength parameters	not	2D
(Zabala and Alonso, 2011)	two-phase single-point	GeoPart	MC-SS	dam construction	not	2D
(Llano-Serna et al., 2015)	one-phase single-point	NairnMPM	VM	gravity	not	2D
(Llano-Serna et al., 2015)	one-phase single-point	NairnMPM	VM	gravity	not	2D

(*continued on next page*)

Table A2 (*continued*)

Citation	Formulation	Code	Constitutive models	Simulated triggering factors	**Contact algorithm?**	**2D/ 3D**
(Yerro et al., 2015)	three-phase single-point	Anura3D	MC-SS	pressure BC	not	2D
(Soga et al., 2016)	two-phase single-point	Anura3D	MC-SS	pressure BC	not	2D
(Yerro et al., 2016b)	two-phase single-point	Anura3D	MCSS	increase of water level inside the slope (updating the hydrostatic distribution of pore pressure)	yes (Bardenhagen)	2D
(Li et al., 2016)	one-phase single-point	MPM3D	MC	gravity	no	2D
(Bhandari et al., 2016)	one-phase single-point	Anura3D	MC	seismic BC (velocity time history)	yes (Bardenhagen)	2D
(Septian et al., 2017)	one-phase single-point	NairnMPM	VM	gravity	no	3D
(Yerro et al., 2018)	one-phase single-point	Anura3D	T	reduction of shear strength parameters	Yes (Bardenhagen)	2D
(Pinyol et al., 2018)	two-phase single-point	Geopart	MC-SS	increase of water level inside the slope (updating the hydrostatic distribution of pore pressure)	no	2D
(Conte et al., 2019)	one-phase single-point	Anura3D	MC-SS	reduction of shear strength parameters	not	2D
(Tran and Sołowski, 2019)	one-phase single-point	Uintah	T-SS-SR	excavation	not	2D
(Shi et al., 2019)	one-phase single-point	MPM3D	DP-SS	reduction of shear strength parameters	yes (Bardenhagen)	2D
(Xu et al., 2019)	one-phase single-point	in-house	DP+R	gravity	no	3D
(Alvarado et al., 2019)	two-phase single-point + thermal effects	Geopart	MC-SS-SR	update of water pressure from FEM analysis	no	2D
(Müller and Vargas, 2019)	two-phase single-point	not stated	MC+R	rock boulder impact	no	2D
(Troncone et al., 2020)	two-phase single-point	Anura3D	MC	reduction of shear strength parameters	not	2D
(Pinyol et al., 2020)	two-phase single-point	Geopart	MC-SS-SR	seismic BC (velocity time history)	no	2D
(Conte et al., 2020)	two-phase single-point	Anura3D	T-SS	reduction of shear strength parameters	no	2D
(Mei et al., 2020)	two-phase single-point	MPM3D	DP-SS	gravity	yes (Bardenhagen)	2D
(Shi et al., 2020)	one-phase single-point	Anura3D	MC	gravity	yes (Bardenhagen)	2D
(Ceccato et al., 2020)	two-phase single point with suction	Anura3D	MC	pressure BC	no	2D
(Liu et al., 2020)	two-phase single point with suction	not stated	DP	infiltration BC	no	2D
(Cuomo et al., 2021)	two-phase single point with suction	Anura3D	MC	infiltration BC	yes (Bardenhagen), not at the failure surface	2D
(Li et al., 2021a, b)	one-phase single-point	MPM3D	DP-SS	gravity (not clear how initial stress state is generated)	yes, contact algorithm improved for velocity weakening friction law	2D
(Ying et al., 2021)	one-phase single-point	not stated	DP-SS	gravity (not clear how initial stress state is generated)	no	2D
(Du et al., 2021)	two-phase double-point	not stated	DP	gravity	no	2D
(Feng et al., 2021)	two-phase double-point	in-house	MC-SS	seismic BC (applied viscous stress at MP)	no	2D
(Zhao et al., 2021)	one-phase single-point	not stated	DP-SS	gravity	no	3D
(Feng and Xu, 2021)	one-phase single-point	CoSim-MPM	DP	reduction of shear strength parameters	no	3D
(Kularathna et al., 2021)	two-phase single-point	GB-geo	MC-SS	pressure BC	no	2D
(Alonso, 2021)	two-phase single-point	Anura3D	MC-SS, T	reduction of shear strength parameters	no	2D
(Troncone et al., 2022)	one-phase single-point	Anura3D	MC-SS	excavation	no	2D
(Yang et al., 2022)	one-phase single-point	in-house	MC	not stated	yes (not stated the theory)	2D
(Nguyen et al., 2022)	two-phase single-point	Anura3D	MC	reduction of shear strength parameters	no	2D
(Kohler and Puzrin, 2022)	one-phase single-point	in-house	MC-SR, LE	seismic BC (traction time-history)	no	2D
(Zhu et al., 2022)	one-phase single-point	MPM3D	MC	reduction of shear strength parameters	no	2D
(Feng et al., 2022)	one-phase single-point	in-house	MC-SS	equivalent nodal forces mapped from SEM calculation	no	3D
(Yeh et al., 2022)	one-phase single-point	Anura3D	MC, MC-SS	reduction of shear strength parameters	no	2D
(Troncone et al., 2023a)	one-phase single-point	Anura3D	T-SS, MC	reduction of shear strength parameters	no	2D
(He et al., 2023)	two-phase single point with suction	Anura3D	MC	rainfall BC	yes (Bardenhagen)	2D
(Zhang et al., 2023a)	one-phase single-point	not stated	DP	not stated	yes, new contact algorithm	3D
(Du et al., 2023)	two-phase double-point	not stated	MC	removal of initial constraint	yes, new contact algorithm	2D
(Liu et al., 2023)	one-phase single-point	Anura3D	T-SS	reduction of shear strength parameters	no	2D
(Lino Ramírez et al., 2023)	two-phase single-point	Anura3D	SANISAND	pressure BC	no	2D
(Zhao et al., 2023)	one-phase single-point	not stated	DP	removal of initial constraint	yes, new contact algorithm	3D
(Zhang et al., 2023b).	one-phase single-point	MPM3D	DP-SS	not stated	yes (not stated the theory)	3D

(*continued on next page*)

Table A2 (*continued*)

Citation	Formulation	Code	Constitutive models	Simulated triggering factors	**Contact algorithm?**	**2D/ 3D**
(Yamaguchi et al., 2023)	two-phase single point with suction	not stated	DP+R	infiltration BC	no	3D
(Kohler et al., 2023)	one-phase single-point	in-house	MC, VP	boundary traction	no	2D
(Troncone et al., 2023b)	one-phase single-point	Anura3D	T	reduction of shear strength parameters	no	2D
(Wu et al., 2023)	one-phase single-point	not stated	MC	not stated	yes, frictional contact	2D
(Du et al., 2023)	one-phase single-point	MPM3D	MC	reduction of shear strength parameters	no	3D
(Fernández et al., 2023)	one-phase single-point	MPM-PUCRio	MCSS	seismic BC (velocity time history)	yes, frictional contact	3D
(Macedo et al., 2024)	two-phase single-point	Anura3D	MC, MC-SS, T	reduction of shear strength parameters and excavation	no	2D
(Di Carluccio et al., 2024)	two-phase single point with suction	Anura3D	Ta-Ger	pressure BC	no	2D
(Tang et al., 2024)	two-phase single point with suction	in-house	DP-SS	infiltration BC	no	2D
(Li et al., 2024)	two-phase single-point	not stated	MC-SS	pressure BC	no	2D
(Zhao et al., 2024)	one-phase single-point	in-house	nonlocal R	gravity	no	3D

References

Abe, K., Soga, K., Bandara, S., 2013. Material point method for coupled hydromechanical problems. J. Geotech. Geoenviron. Eng. 140, 1–16. https://doi.org/10.1061/(ASCE)GT.1943-5606.0001011.

Alonso, E.E., 2021. Triggering and motion of landslides. Geotechnique 71, 3–59. https://doi.org/10.1680/jgeot.20.RL.001.

Alsardi, A., Yerro, A., 2023. Coseismic site response and slope instability using periodic boundary conditions in the material point method. J. Rock Mech. Geotech. Eng. 15, 641–658. https://doi.org/10.1016/j.jrmge.2022.09.016.

Alvarado, M., Pinyol, N.M., Alonso, E.E., 2019. Landslide motion assessment including rate effects and thermal interactions: Revisiting the canelles landslide. Can. Geotech. J. 56, 1338–1350. https://doi.org/10.1139/cgj-2018-0779.

Andersen, S., 2009. Material-Point Analysis of Large-Strain Problems: Modelling of Landslides. AAlborg University.

Andersen, S., Andersen, L., 2010. Modelling of landslides with the material-point method. Comput. Geosci. 14, 137–147. https://doi.org/10.1007/s10596-009-9137-y.

Augarde, C.E., Lee, S.J., Loukidis, D., 2021. Numerical modelling of large deformation problems in geotechnical engineering: A state-of-the-art review. Soils Found. 61, 1718–1735. https://doi.org/10.1016/j.sandf.2021.08.007.

Aviles, L.A., Di, G., Pinyol, N.M., 2024. Computers and geotechnics layered construction process with the material point method. Comput. Geotech. 171 https://doi.org/10.1016/j.compgeo.2024.106401.

Bandara, S., Soga, K., 2015. Coupling of soil deformation and pore fluid flow using material point method. Comput. Geotech. 63, 199–214. https://doi.org/10.1016/j.compgeo.2014.09.009.

Bardenhagen, S., Kober, E., 2004. The generalized interpolation material point method. Comput. Model. Eng. Sci. 5, 477–495.

Bardenhagen, S.G., Guilkey, J.E., Roessig, K.M., Brackbill, J.U., Witzel, W.M., Foster, J. C., 2001. An improved contact algorithm for the material point method and application to stress propagation in granular material. C. Comput. Model. Eng. Sci. 2, 509–522.

Bhandari, T., Hamad, F., Moormann, C., Sharma, K.G., Westrich, B., 2016. Numerical modelling of seismic slope failure using MPM. Comput. Geotech. 75, 126–134. https://doi.org/10.1016/j.compgeo.2016.01.017.

Burghardt, J., Brannon, R., Guilkey, J., 2012. A nonlocal plasticity formulation for the material point method. Comput. Methods Appl. Mech. Eng. 225–228, 55–64. https://doi.org/10.1016/j.cma.2012.03.007.

Ceccato, F., 2014. Study of Large Deformation Geomechanical Problems with the Material Point Method. Ph.D. thesis. University of Padua, Italy.

Ceccato, F., Simonini, P., 2016. Granular flow impact forces on protection structures: MPM numerical simulations with different constitutive models. Procedia Eng. 158, 164–169. https://doi.org/10.1016/j.proeng.2016.08.423.

Ceccato, F., Simonini, P., 2019. Numerical features used in simulations. In: Fern, J., Rohe, A., Soga, K., Alonso, E. (Eds.), The Material Point Method for Geotechnical Engineering. CRC Press, pp. 101–124. https://doi.org/10.1201/9780429028090-6.

Ceccato, F., Beuth, L., Simonini, P., 2017. Adhesive contact algorithm for MPM and its application to the simulation of cone penetration in clay. Process. Eng. 182–188. https://doi.org/10.1016/j.proeng.2017.01.004.

Ceccato, F., Cola, S., Girardi, V., Simonini, P., 2020. Effect of artificial snowing system on the stability of a Ski slope in the Dolomites. In: Cabrera, M.A., Prada-Sarmiento, L.F., Montero, J. (Eds.), SCG-XIII International Symposium on Landslides.

Ceccato, F., Lu, M., Camporese, M., Vallisari, D., 2023. Simulation of rainfall-induced landslides from small to large displacements with an efficient sequential use of FEM and MPM. In: Ferrari, A., Rosone, M., Ziccarelli, M., Gottardi, G. (Eds.), Geotechnical Engineering in the Digital and Technological Innovation Era. CNRIG 2023. Springer, Palermo, Italy, pp. 419–426. https://doi.org/10.1007/978-3-031-34761-0_51.

Chen, H., Hagiwara, I., Tieu, A.K., 2011. A seamless coupling between molecular dynamics and material point method. Jpn. J. Ind. Appl. Math. 28, 55–67. https://doi.org/10.1007/s13160-011-0026-0.

Chen, Z.P., Qiu, X.M., Zhang, X., Lian, Y.P., 2015. Improved coupling of finite element method with material point method based on a particle-to-surface contact algorithm. Comput. Methods Appl. Mech. Eng. 293, 1–19. https://doi.org/10.1016/j.cma.2015.04.005.

Coetzee, C.J., 2005. The Material Point Method. Stellenbosh, South Africa.

Conte, E., Pugliese, L., Troncone, A., 2019. Post-failure stage simulation of a landslide using the material point method. Eng. Geol. 253, 149–159. https://doi.org/10.1016/j.enggeo.2019.03.006.

Conte, E., Pugliese, L., Troncone, A., 2020. Post-failure analysis of the Maierato landslide using the material point method. Eng. Geol. 277, 105788 https://doi.org/10.1016/j.enggeo.2020.105788.

Cundall, P.A., Strack, O.D.L., 1979. A discrete numerical model for granular assemblies. Geotechnique 29, 47–65.

Cuomo, S., Di Perna, A., Martinelli, M., 2021. Modelling the spatio-temporal evolution of a rainfall-induced retrogressive landslide in an unsaturated slope. Eng. Geol. 294, 106371 https://doi.org/10.1016/j.enggeo.2021.106371.

Di Carluccio, G., Pinyol, N.M., Alonso, E.E., Hürlimann, M., 2024. Liquefaction-induced flow-like landslides. The case of Valarties (Spain). Geotechnique 74, 307–324. https://doi.org/10.1680/jgeot.21.00112.

Dong, Y., Wang, D., Randolph, M.F., 2017. Investigation of impact forces on pipeline by submarine landslide using material point method. Ocean Eng. 146, 21–28. https://doi.org/10.1016/j.oceaneng.2017.09.008.

Du, W., Sheng, Q., Fu, X., Chen, J., Zhou, Y., 2021. Extensions of the two-phase double-point material point method to simulate the landslide-induced surge process. Eng. Anal. Bound. Elem. 133, 362–375. https://doi.org/10.1016/j.enganabound.2021.09.020.

Du, W., Sheng, Q., Fu, X., Chen, J., Wei, P., Zhou, Y., 2023. Post-failure analysis of landslide blocking river using the two-phase double-point material point method: a case of western Hubei, China. Bull. Eng. Geol. Environ. 82, 1–18. https://doi.org/10.1007/s10064-023-03122-6.

Feng, Z.K., Xu, W.J., 2021. GPU material point method (MPM) and its application on slope stability analysis. Bull. Eng. Geol. Environ. 80, 5437–5449. https://doi.org/10.1007/s10064-021-02265-8.

Feng, K., Huang, D., Wang, G., 2021a. Two-layer material point method for modeling soil – water interaction in unsaturated soils and rainfall-induced slope failure. Acta Geotech. 9 https://doi.org/10.1007/s11440-021-01222-9.

Feng, K., Wang, G., Huang, D., Jin, F., 2021b. Material point method for large-deformation modeling of coseismic landslide and liquefaction-induced dam failure. Soil Dyn. Earthq. Eng. 150, 106907 https://doi.org/10.1016/j.soildyn.2021.106907.

Feng, K., Huang, D., Wang, G., Jin, F., Chen, Z., 2022. Physics-based large-deformation analysis of coseismic landslides: A multiscale 3D SEM-MPM framework with application to the Hongshiyan landslide. Eng. Geol. 297, 106487 https://doi.org/10.1016/j.enggeo.2021.106487.

Fern, E.J.J., Soga, K., 2016. the role of constitutive models in MPM simulations of granular column collapses. Acta Geotech. 11, 659–678. https://doi.org/10.1007/s11440-016-0436-x.

Fern, E.J., Rohe, A., Soga, K., Alonso, E.E., 2019. The Material Point Method for Geotechnical Engineering: A Practical Guide. CRC Press.

Fernández, F., Vargas, E., Muller, A.L., Sousa, R.L., eSousa, L.R., 2023. Material point method modeling in 3D of the failure and run-out processes of the Daguangbao landslide. Acta Geotech. 4 https://doi.org/10.1007/s11440-023-02152-4.

Gaume, J., Puzrin, A.M., 2021. Mechanisms of slab avalanche release and impact in the Dyatlov Pass incident in 1959. Commun. Earth Environ. 2 https://doi.org/10.1038/s43247-020-00081-8.

González Acosta, J.L., Vardon, P.J., Hicks, M.A., 2021b. Study of landslides and soil-structure interaction problems using the implicit material point method. Eng. Geol. 285 https://doi.org/10.1016/j.enggeo.2021.106043.
González Acosta, J.L., Vardon, P.J., Hicks, M.A., 2021a. Development of an implicit contact technique for the material point method. Comput. Geotechn. 130 https://doi.org/10.1016/j.compgeo.2020.103859.
Guilkey, J., Weiss, J., 2001. An implicit time integration strategy for use with the material point method. In: Proceedings from the First MIT Conference on Computational Fluid and Solid Mechanics.
Guilkey, J.E., Weiss, J.A., 2003. Implicit time integration for the material point method: quantitative and algorithmic comparisons with the finite element method. Int. J. Numer. Methods Eng. 57, 1323–1338. https://doi.org/10.1002/nme.729.
He, K., Xi, C., Liu, B., Hu, X., Luo, G., Ma, G., Zhou, R., 2023. MPM-based mechanism and runout analysis of a compound reactivated landslide. Comput. Geotech. 159, 105455 https://doi.org/10.1016/j.compgeo.2023.105455.
Hu, W., Chen, Z., 2003. A multi-mesh MPM for simulating the meshing process of spur gears. Comput. Struct. 81, 1991–2002. https://doi.org/10.1016/S0045-7949(03)00260-8.
Iaconeta, I., Larese, A., Rossi, R., Oate, E., 2017. An implicit material point method applied to granular flows. Procedia Eng. 175, 226–232. https://doi.org/10.1016/j.proeng.2017.01.017.
Idelsohn, S.R., Oñate, E., Del Pin, F., 2003. A Lagrangian meshless finite element method applied to fluid–structure interaction problems. Comput. Struct. 81, 655–671. https://doi.org/10.1016/S0045-7949(02)00477-7.
Jassim, I., Stolle, D., Vermeer, P.A., 2013. Two-phase dynamic analysis by material point method. Int. J. Numer. Anal. Methods Geomech. 37, 2502–2522. https://doi.org/10.1002/nag.2146.
Kakouris, E.G., Triantafyllou, S.P., 2017. Phase-field material point method for brittle fracture. Int. J. Numer. Methods Eng. 112, 1750–1776. https://doi.org/10.1002/nme.5580.
Kohler, M., Puzrin, A.M., 2022. Mechanism of co-seismic deformation of the slow-moving La Sorbella landslide in Italy revealed by MPM analysis. Case Rep. Med. 127, 1–25. https://doi.org/10.1029/2022JF006618.
Kohler, M., Hodel, D., Keller, L., Molinari, A., Puzrin Alexander, M.C., 2023. Case Study of an Active Landslide at the Flank of a Water Reservoir and its Response during Earthquakes.
Kularathna, S., Liang, W., Zhao, T., Chandra, B., Zhao, J., Soga, K., 2021. A semi-implicit material point method based on fractional-step method for saturated soil. Int. J. Numer. Anal. Methods Geomech. 45, 1405–1436. https://doi.org/10.1002/nag.3207.
Lambe, T.W., 1973. Predictions in soil engineering. Géotechnique 23, 151–202.
Lei, X., He, S., Chen, X., Wong, H., Wu, L., Liu, E., 2020. A generalized interpolation material point method for modelling coupled seepage-erosion-deformation process within unsaturated soils. Adv. Water Res. 141, 103578. https://doi.org/10.1016/j.advwatres.2020.103578.
Li, S., Liu, W.K., 2002. Meshfree and particle methods and their applications. Appl. Mech. Rev. 55, 1. https://doi.org/10.1115/1.1431547.
Li, X., Wu, Y., He, S., Su, L., 2016. Application of the material point method to simulate the post-failure runout processes of the Wangjiayan landslide. Eng. Geol. 212, 1–9. https://doi.org/10.1016/j.enggeo.2016.07.014.
Li, Xingyue, Sovilla, B., Jiang, C., Gaume, J., 2021a. Three-dimensional and real-scale modeling of flow regimes in dense snow avalanches. Landslides 18, 3393–3406. https://doi.org/10.1007/s10346-021-01692-8.
Li, Xinpo, Tang, X., Zhao, S., Yan, Q., Wu, Y., 2021b. MPM evaluation of the dynamic runout process of the giant Daguangbao landslide. Landslides 18, 1509–1518. https://doi.org/10.1007/s10346-020-01569-2.
Li, Y., Zhang, J.M., Wang, R., 2024. An explicit material point and finite volume sequentially coupled method for simulating large deformation problems in saturated soil. Comput. Geotech. 170, 106270 https://doi.org/10.1016/j.compgeo.2024.106270.
Liang, W., Zhao, J., 2019. Multiscale modeling of large deformation in geomechanics. Int. J. Numer. Anal. Methods Geomech. 43, 1080–1114. https://doi.org/10.1002/nag.2921.
Liang, Y., Benedek, T., Zhang, X., Liu, Y., 2017. Material point method with enriched shape function for crack problems. Comput. Methods Appl. Mech. Eng. 322, 541–562. https://doi.org/10.1016/j.cma.2017.05.012.
Liang, Y., Chandra, B., Soga, K., 2022. Shear band evolution and post-failure simulation by the extended material point method (XMPM) with localization detection and frictional self-contact. Comput. Methods Appl. Mech. Eng. 390, 114530 https://doi.org/10.1016/j.cma.2021.114530.
Lino Ramírez, E., Taiebat, M., Lizcano, A., 2023. Flow liquefaction and large deformation analysis in a tailings dam using MPM and critical state-based material modelling. In: Zdravkovic, L., Kontoe, S., Taborda, D.M.G. (Eds.), 10th European Conference on Numerical Methods in Geotechnical Engineering, pp. 1–6. London (UK).
Liu, C., Sun, Q., Jin, F., Zhou, G.G.D., 2017. A fully coupled hydro-mechanical material point method for saturated dense granular materials. Powder Technol. 314, 110–120. https://doi.org/10.1016/j.powtec.2017.02.022.
Liu, X., Wang, Y., Li, D.Q., 2020. Numerical simulation of the 1995 rainfall-induced Fei Tsui Road landslide in Hong Kong: new insights from hydro-mechanically coupled material point method. Landslides 17, 2755–2775. https://doi.org/10.1007/s10346-020-01442-2.
Liu, Z.Q., Zhou, M.L., Lu, M., Dibiagio, A., Heyerdahl, H., 2023. Numerical simulation for runout behaviour of sensitive clay landslides using the material point method. In: Zdravkovic, L., Kontoe, S., Taborda, D.M.G., T.A. (Eds.), 10th European Conference on Numerical Methods in Geotechnical Engineering, pp. 1–6. London (UK).
Llano-Serna, M.A., Farias, M.M., Pedroso, D., 2015. An assessment of the material point method for modelling large scale run-out processes in landslides. Landslides. https://doi.org/10.1007/s10346-015-0664-4.
Lu, M., Girardi, V., Zhou, M., Ceccato, F., 2023. A new strategy for the initialization of MPM simulations. In: Zdravkovi, L., S, K., DMG, T., A, T (Eds.), Proceedings 10th NUMGE 2023. London (UK).
Ma, J., Wang, D., Randolph, M.F., 2014. A new contact algorithm in the material point method for geotechnical simulations. Int. J. Numer. Anal. Methods Geomech. 1197–1210 https://doi.org/10.1002/nag.
Macedo, J., Yerro, A., Cornejo, R., Pierce, I., 2024. Cadia TSF failure assessment considering triggering and post-triggering mechanisms. J. Geotech. Geoenviron. Eng. 150 (4) https://doi.org/10.1061/JGGEFK.GTENG-11660.
Martinelli, M., 2016. Soil-Water Interaction with Material Point Method. Double-Point Formulation.
Mei, X., Ma, G., Hu, X., Shi, B., Huang, D., 2020. Simulation of the failure process of submarine landslides on a seabed by coupled MPM. J. Coast. Res. 111, 231–237. https://doi.org/10.2112/JCR-SI111-041.1.
Mieremet, M.M.J.M.J., Stolle, D.F.F., Ceccato, F., Vuik, C., 2015. Numerical stability for modelling of dynamic two-phase interaction. Int. J. Numer. Anal. Methods Geomech. 40 https://doi.org/10.1002/nag.2483.
Monaghan, J.J., 2012. Smoothed Particle Hydrodynamics and its Diverse applications. Annu. Rev. Fluid Mech. 44, 323–346. https://doi.org/10.1146/annurev-fluid-120710-101220.
Moresi, L., Dufour, F., Muhlhous, H.-B., 2003. A Lagrangian integration point finite element method for large deformation modelling of viscoelastic geomaterials. J. Comput. Phys. 184, 476–497.
Müller, A., Vargas, E.A., 2019. Stability analysis of a slope under impact of a rock block using the generalized interpolation material point method (GIMP). Landslides 16, 751–764. https://doi.org/10.1007/s10346-018-01131-1.
Nairn, J.A., 2019. Modeling heat flow across material interfaces and cracks using the material point method. Comput. Part. Mech. 6, 133–144. https://doi.org/10.1007/s40571-018-0201-z.
Nguyen, T.S., Yang, K.H., Wu, Y.K., Teng, F., Chao, W.A., Lee, W.L., 2022. Post-failure process and kinematic behavior of two landslides: case study and material point analyses. Comput. Geotech. 148, 104797 https://doi.org/10.1016/j.compgeo.2022.104797.
Pinyol, N.M., Alvarado, M., Alonso, E.E., Zabala, F., 2018. Thermal effects in landslide mobility. Géotechnique 68, 528–545. https://doi.org/10.1680/jgeot.17.P.054.
Pinyol, N.M., Alvarado, M., Garcia, L.M., 2020. Dynamics of slow and fast landslides. Int. Soc. Soil Mech. Geotech. Eng. SCG-XIII I, 536–537.
Qiu, G., Henke, S., Grabe, J., 2011. Application of a Coupled Eulerian–Lagrangian approach on geomechanical problems involving large deformations. Comput. Geotech. 38, 30–39. https://doi.org/10.1016/j.compgeo.2010.09.002.
Qu, C. Xiang, Wang, G., Feng, K. Wei, Xia, Z. Dong, 2021. Large deformation analysis of slope failure using material point method with cross-correlated random fields. J. Zhejiang Univ. Sci. A 22, 856–869. https://doi.org/10.1631/jzus.A2100196.
Remmerswaal, G., Vardon, P.J., Hicks, M.A., 2021. Evaluating residual dyke resistance using the Random Material Point Method. Comput. Geotech. 133, 104034 https://doi.org/10.1016/j.compgeo.2021.104034.
Sadeghirad, A., Brannon, R.M., Burghardt, J., 2011. Aconvected Particle Domain Interpolation Technique to Extend Applicability of the Material Point Method for Problems Involving Massive Deformations, pp. 1435–1456. https://doi.org/10.1002/nme.
Septian, A., Llano-Serna, M.A., Ruest, M.R., Williams, D.J., 2017. Three-dimensional kinematic analysis of Bingham Canyon mine pit wall slides. Procedia Eng. 175, 86–93. https://doi.org/10.1016/j.proeng.2017.01.030.
Shi, B., Zhang, Y., Zhang, W., 2019. Run-out of the 2015 Shenzhen landslide using the material point method with the softening model. Bull. Eng. Geol. Environ. 78, 1225–1236. https://doi.org/10.1007/s10064-017-1167-4.
Shi, J.J., Zhang, W., Wang, B., Li, C.Y., Pan, B., 2020. Simulation of a submarine landslide using the coupled material point method. Math. Probl. Eng. 2020 https://doi.org/10.1155/2020/4392581.
Soga, K., Alonso, E., Yerro, A., Kumar, K., Bandara, S., 2016. Trends in large-deformation analysis of landslide mass movements with particular emphasis on the material point method. Géotechnique 66, 248–273. https://doi.org/10.1680/jgeot.15.LM.005.
Sołowski, W.T., Berzins, M., Coombs, W.M., Guilkey, J.E., Möller, M., Tran, Q.A., Adibaskoro, T., Seyedan, S., Tielen, R., Soga, K., 2021. Material point method: overview and challenges ahead. Adv. Appl. Mech. 54, 113–204. https://doi.org/10.1016/bs.aams.2020.12.002.
Steffen, M., Wallstedt, P.C., Guilkey, J.E., Kirby, R.M., Berzins, M., 2008. Examination and analysis of implementation choices within the Material Point Method (MPM). C. Comput. Model. Eng. Sci. 31, 107–127. https://doi.org/10.3970/cmes.2008.031.107.
Stomakhin, A., Schroeder, C., Jiang, C., Chai, L., Teran, J., Selle, A., 2014. Augmented MPM for phase-change and varied materials. ACM Trans. Graph. 33, 1–11. https://doi.org/10.1145/2601097.2601176.
Sulsky, D., Chen, Z., Schreyer, H.L., 1994. A particle method for hystory-dependent materials. Comput. Methods Appl. Mech. Eng. 118, 179–196.
Sulsky, D., Zhou, S.-J., Schreyer, H.L., 1995. Application of a particle-in-cell method to solid mechanics. Comput. Phys. Commun. 87, 236–252. https://doi.org/10.1016/0010-4655(94)00170-7.
Tang, X., Li, X., He, S., 2024. A stabilized two-phase material point method for hydromechanically coupled large deformation problems. Bull. Eng. Geol. Environ. 83, 1–19. https://doi.org/10.1007/s10064-024-03668-z.
Tran, Q.A., Sołowski, W., 2019. Generalized Interpolation Material Point Method modelling of large deformation problems including strain-rate effects – Application

to penetration and progressive failure problems. Comput. Geotech. 106, 249–265. https://doi.org/10.1016/j.compgeo.2018.10.020.
Tran, Q.A., Sørlie, E.R., Grimstad, G., Eiksund, G.R., 2023. Role of hydraulic conductivity on the mechanism of earthquake induced submarine landslides – a CFD-MPM analysis. In: Zdravkovic, L., Kontoe, S., Taborda, D.M. (Eds.), 10th European Conference on Numerical Methods in Geotechnical Engineering. London (UK), pp. 2–7.
Troncone, A., Pugliese, L., Conte, E., 2020. Run-out simulation of a landslide triggered by an increase in the groundwater level using the material point method. Water (Switzerland) 12 (10). https://doi.org/10.3390/w12102817.
Troncone, A., Pugliese, L., Conte, E., 2022. Analysis of an excavation-induced landslide in stiff clay using the material point method. Eng. Geol. 296, 106479 https://doi.org/10.1016/j.enggeo.2021.106479.
Troncone, A., Pugliese, L., Parise, A., Conte, E., 2023a. Analysis of a landslide in sensitive clays using the material point method. Geotech. Res. https://doi.org/10.1680/jgere.22.00060.
Troncone, A., Pugliese, L., Parise, A., Conte, E., 2023b. A practical approach for predicting landslide retrogression and run-out distances in sensitive clays. Eng. Geol. 326, 107313 https://doi.org/10.1016/j.enggeo.2023.107313.
Wang, B., Hicks, M.A., Vardon, P.J., 2016. Slope failure analysis using the random material point method. Géotechn. Lett. 6, 113–118. https://doi.org/10.1680/jgele.16.00019.
Wood, D.M., 2004. Geotechnical Modelling. Taylor & Francis, Abingdon, UK. https://doi.org/10.4324/9780203477977.
Wu, F., Sun, W., Li, X., Guan, Y., Dong, M., 2023. Material point method-based simulation of dynamic process of soil landslides considering pore fluid pressure. Int. J. Numer. Anal. Methods Geomech. 47, 2385–2404. https://doi.org/10.1002/nag.3581.
Xu, X., Jin, F., Sun, Q., Soga, K., Zhou, G.G.D., 2019. Three-dimensional material point method modeling of runout behavior of the Hongshiyan landslide. Can. Geotech. J. 56, 1318–1337. https://doi.org/10.1139/cgj-2017-0638.
Yamaguchi, Y., Makinoshima, F., Oishi, Y., 2023. Simulating the entire rainfall-induced landslide process using the material point method for unsaturated soil with implicit and explicit formulations. Landslides 20, 1617–1638. https://doi.org/10.1007/s10346-023-02052-4.
Yang, Y., Wang, R., Xu, W., Wang, Y., Yan, L., 2022. Characterization of the kinematic evolution of the hongshiyan landslide using the material point method. Front. Phys. 10, 1–14. https://doi.org/10.3389/fphy.2022.829262.
Yeh, F.H., Lai, Y.C., Ge, L., Cheng, S.H., 2022. Evaluation of the material point method in modeling the post-failure and run-out of translational landslide: a case study in Taiwan. J. Test. Eval. 50, 1–21. https://doi.org/10.1520/JTE20210791.
Yerro, A., 2015. MPM Modelling of Landslides in Brittle and Unsaturated Soils. Ph.D thesis. Univestitat Politecnica de Catalunya, Spain.
Yerro, A., Alonso, E.E., Pinyol, N.M.M., 2015. The material point method for unsaturated soils. Geotechnique 65, 201–217. https://doi.org/10.1680/geot.14.P.163.
Yerro, A., Alonso, E.E., Pinyol, N., 2016a. Modelling large deformation problems in unsaturated soils, in: E-UNSAT 2016a. pp. 1–6. doi:https://doi.org/10.1051/e3sconf/20160908019.
Yerro, A., Alonso, E.E., Pinyol, N.M., 2016b. Run-out of landslides in brittle soils. Comput. Geotech. Geotech. 1–13 https://doi.org/10.1016/j.compgeo.2016.03.001.
Yerro, A., Pinyol, N.M., Alonso, E.E., 2016c. Internal progressive failure in deep-seated landslides. Rock Mech. Rock. Eng. 49, 2317–2332. https://doi.org/10.1007/s00603-015-0888-6.
Yerro, A., Soga, K., Bray, J., 2018. Runout evaluation of Oso landslide with the material point method. Can. Geotech. J. 14, 1–14. https://doi.org/10.1139/cgj-2017-0630.
Yerro, A., Girardi, V., Ceccato, F., Martinelli, M., 2022. Modelling unsaturated soils with the Material Point Method. A discussion of the state-of-the-art. Geomech. Energy Environ. 32, 100343 https://doi.org/10.1016/j.gete.2022.100343.
Ying, C., Zhang, K., Wang, Z.N., Siddiqua, S., Makeen, G.M.H., Wang, L., 2021. Analysis of the run-out processes of the Xinlu Village landslide using the generalized interpolation material point method. Landslides 18, 1519–1529. https://doi.org/10.1007/s10346-020-01581-6.
Yu, H.S., 1993. Discussion: singular plastic fields in steady penetration of a rigid cone. J. Appl. Mech. 60, 1061–1062.
Zabala, F., Alonso, E.E., 2011. Progressive failure of Aznalcóllar dam using the material point method. Géotechnique 61, 795–808. https://doi.org/10.1680/geot.9.P.134.
Zhan, Z.Q., Zhou, C., Liu, C.Q., Ng, C.W.W., 2023. Modelling hydro-mechanical coupled behaviour of unsaturated soil with two-phase two-point material point method. Comput. Geotech. 155 https://doi.org/10.1016/j.compgeo.2022.105224.
Zhang, D.Z., Ma, X., Giguere, 2011. Material point method enhanced by modified gradient of shape function. Journal of Computational Physics 230 (16), 6379–6398. https://doi.org/10.1016/j.jcp.2011.04.032.
Zhang, W., Wu, Z., Peng, C., Li, S., Dong, Y., Yuan, W., 2023a. Modelling large-scale landslide using a GPU-accelerated 3D MPM with an efficient terrain contact algorithm. Comput. Geotech. 158, 105411 https://doi.org/10.1016/j.compgeo.2023.105411.
Zhang, R., Xue, X., Deng, C., 2023b. Investigation of motion characteristics of catastrophic landslide using material point method and gene expression programming. Int. J. Rock Mech. Min. Sci. 170, 105507 https://doi.org/10.1016/j.ijrmms.2023.105507.
Zhao, J., Chen, Y., Zhang, H., Xia, H., Wang, Z., Peng, Q., 2019. Physically based modeling and animation of landslides with MPM. Vis. Comput. 35, 1223–1235. https://doi.org/10.1007/s00371-019-01709-3.
Zhao, S., He, S., Li, X., Deng, Y., Liu, Y., Yan, S., Bai, X., Xie, Y., 2021. The Xinmo rockslide-debris avalanche: an analysis based on the three-dimensional material point method. Eng. Geol. 287, 106109 https://doi.org/10.1016/j.enggeo.2021.106109.
Zhao, S., Zhu, L., Liu, W., Li, X., He, S., Scaringi, G., Tang, X., Liu, Y., 2023. Substratum virtualization in three-dimensional landslide modeling with the material point method. Eng. Geol. 315, 107026 https://doi.org/10.1016/j.enggeo.2023.107026.
Zhao, S., He, S., Li, X., Scaringi, G., Liu, Y., Deng, Y., 2024. Investigating the dynamic process of a rock avalanche through an MLS-MPM simulation incorporated with a nonlocal μ(I) rheology model. Landslides. https://doi.org/10.1007/s10346-024-02244-6.
Zhu, Y., Ishikawa, T., Zhang, Y., Nguyen, B.T., Subramanian, S.S., 2022. A FEM-MPM hybrid coupled framework based on local shear strength method for simulating rainfall/runoff-induced landslide runout. Landslides 19, 2021–2032. https://doi.org/10.1007/s10346-022-01849-z.
Zienkiewicz, O.C., Chan, A.H.C., Pastor, M., Schrefler, B.A., Shiomi, T., 1999. Computational Geomechanics, Engineering. Wiley & Sons, New York.

Further reading

Zhao, Y., Choo, J., 2020. Stabilized material point methods for coupled large deformation and fluid flow in porous materials. Comput. Methods Appl. Mech. Eng. 362, 112742 https://doi.org/10.1016/j.cma.2019.112742.